Stabilization and decay rate estimation of nonlinear flexible marine riser system with the rotational inertia under nonlinear boundary controls

Yi Cheng, Yuexi Zhang, Yuhu Wu, *Member, IEEE* and Bao-Zhu Guo, *Senior member, IEEE*

***Abstract*—This paper investigates the boundary stabilization of a flexible marine riser system that takes rotational inertia into account. This system is described using a nonlinear partial differential equation under the nonlinear controls. Specifically, we focus on applying nonlinear boundary feedback control forces and torques at the top end of the riser. Utilizing measurements of boundary velocity and angular velocity, we devise nonlinear feedback mechanisms aimed at mitigating vibrations within the flexible marine riser system. Our approach encompasses a broad range of nonlinear feedback scenarios. To establish the well-posedness of the resulting closed-loop system, we employ the nonlinear semigroup method. Furthermore, we leverage the integral multiplier technique to demonstrate that the stability characteristics of the closed-loop system are dictated by a dissipative ordinary differential equation. As the nonlinear feedback functions exhibit distinct growth patterns in proximity to the origin, we identify three primary types of decay behaviors. These are subsequently estimated through solutions of the ordinary differential equation and validated through numerical simulations.**

***Index Terms*—Nonlinear flexible marine riser, nonlinear boundary control, well-posedness, stability.**

I. Introduction

A. Background

Vibration control for flexible systems has garnered significant attention over the decades owing to its diverse engineering applications. Notably, flexible manipulators for grasping [34], marine mooring lines for maintaining stationary positions [19], and marine risers for oil transportation [15] are just a few examples. Depending on the characteristics of the flexible structures, these systems can primarily be classified as string systems [41] or beam systems [8]. Marine riser systems, in particular, are often modeled as beams [18] due to the inherent flexibility of the riser material. In the harsh marine environment, flexible marine risers undergo vibration and torsional deformation, compromising system efficiency and even reducing material lifespan. To mitigate system vibration and enhance overall performance, various control methods have been devised from different viewpoints. These methods encompass, among others, reduced-order modeling [39], robust adaptive control [20], and linear quadratic regulator (LQR) control [40]. Among these, boundary control [14] stands out due to its minimal sensor and actuator requirements and practical ease of implementation, making it a widely adopted approach for stabilizing flexible marine riser systems.

Indeed, the boundary stabilization of flexible marine riser systems, particularly those based on the linear Euler-Bernoulli beam model, has been extensively researched. For instance, in some studies, tension is assumed to be constant [21]. However, in real-world scenarios, most flexible marine riser systems experience tension variations that depend on both time and space. These variations are primarily influenced by factors such as shear deformation, velocity, and large amplitudes, which often result in nonlinear models [14], [18], [22], [42]. Notably, while modeling flexible marine risers, the impact of rotational inertia is frequently overlooked in the aforementioned studies. Nevertheless, considering the characteristics and deformations of the flexible riser during the vibration process, it becomes imperative to account for the influence of rotational inertia [33], [36]. Currently, there are limited published studies focusing on boundary stabilization for nonlinear flexible marine riser systems incorporating rotational inertia.

Motivated by this, in this paper, we develop a model for a nonlinear flexible marine riser system with rotational inertia based on Hamilton's principle. This model is described by

$$\begin{aligned}&\rho\Lambda\Upsilon_{tt}(x,t)-\rho I\Upsilon_{xxtt}(x,t)+\mathcal{E}I\Upsilon_{xxxx}(x,t)\\&=\left[\mathbb{P}(\Upsilon_x(x,t))\Upsilon_x(x,t)\right]_x,\end{aligned}\tag{1}$$

for all $x\in(0,L)$ and $t>0$, where $\Upsilon(x,t)$ represents the position of the flexible marine riser in the XOY coordinate frame at the position x and time t (see, e.g., Fig. 1), $(\cdot)_{xt}=\frac{\partial(\cdot)}{\partial x\partial t}$, $\rho I\Upsilon_{xxtt}(x,t)$ represents the rotational inertia [24]. Additionally, the nonlinear function $\mathbb{P}(\cdot)$ is given by

$$\mathbb{P}(\Upsilon_x(x,t))=\mathcal{E}\Lambda+\frac{P-\mathcal{E}\Lambda}{\sqrt{1+\Upsilon_x^2(x,t)}},\tag{2}$$

which represents the nonlinear tension of the flexible marine riser from the nonlinear geometric relation [27], [28], and $\rho I,\rho\Lambda,\mathcal{E}I,\mathcal{E}\Lambda$ and P represent respectively the vibration

This work was partially supported by National Natural Science Foundation of China (Nos. 62173062,12131008,U23B2033), and Science and Technology Project of Liaoning Provincial Department of Education (No. LJKMZ20221490). The material in this paper was not presented at any conference.

Y. Cheng and Y. Zhang are with School of Mathematical Sciences, Bohai University, Jinzhou, 121013, China (e-mail: chengyi407@bhu.edu.cn; zhangyuexi0110@outlook.com).

Y. Wu is with Key Laboratory of Intelligent Control and Optimization for Industrial Equipment of Ministry of Education, and School of Control Science and Engineering, Dalian University of Technology, Dalian 116024, China (e-mail: wuyuhu@dlut.edu.cn).

B.Z. Guo is with the School of Mathematics and Physics, North China Electric Power University, Beijing 102206, China, and Key Laboratory of System and Control, Academy of Mathematics and Systems Science, Academia Sinica, Beijing 100190 (e-mail: bzguo@iss.ac.cn).

mass, mass moment of inertia of each unit length of the riser, bending stiffness, tensile stiffness, and initial tension. From a physics standpoint, the equation (1) describes the dynamic behavior of a class of nonlinear flexible beams undergoing large-amplitude motion. This general equation encompasses several specialized beam equations as particular cases. Specifically, when the tension changes caused by vibrations during deformation are ignored, that is, when $\mathbb{P}(\Upsilon_x(\cdot,\cdot)) = 0$, the equation (1) simplifies to the Rayleigh beam equation, as referenced in [37]. When the influence of rotational inertia is not taken into account, that is, when $\rho I = 0$, the equation (1) can be simplified into a nonlinear flexible beam equation, as noted in [8]. In the case of beam systems with finite but small amplitudes, this implies that $\frac{1}{\sqrt{1+\Upsilon_x^2(\cdot,\cdot)}} \approx 1 - \frac{1}{2}\Upsilon_x^2(\cdot,\cdot)$ as $\Upsilon_x^2(\cdot,\cdot) \ll 1$, the nonlinear tension given by (2) can be approximated as

$$\mathbb{P}(\Upsilon_x(x,t)) = P + \frac{1}{2}\mathcal{E}\Lambda\Upsilon_x^2(x,t). \tag{3}$$

In this case, an approximate form of equation (1) can be rewritten as follows:

$$\begin{aligned}&\rho\Lambda\Upsilon_{tt}(x,t) - \rho I\Upsilon_{xxtt}(x,t) + \mathcal{E}I\Upsilon_{xxxx}(x,t)\\ &-P\Upsilon_{xx}(x,t) - \frac{3}{2}\mathcal{E}\Lambda\Upsilon_x^2(x,t)\Upsilon_{xx}(x,t) = 0,\end{aligned} \tag{4}$$

which has been studied in [33], [18], [14] and [15] in the context where rotational inertia was neglected, highlights the significance of the nonlinear tension term. However, to the best of our knowledge, there are currently no published results specifically addressing boundary stabilization for this nonlinear flexible marine riser system described by equation (1). The objective of this paper is to mitigate vibrations in the flexible marine riser system described by equation (1) through the application of two boundary control inputs:

$$\begin{cases}\rho I\Upsilon_{xtt}(L,t) + (\mathcal{E}\Lambda + \dfrac{P-\mathcal{E}\Lambda}{\sqrt{1+\Upsilon_x^2(L,t)}})\Upsilon_x(L,t)\\ \quad -\mathcal{E}I\Upsilon_{xxx}(L,t) = U_1(t),\\ \mathcal{E}I\Upsilon_{xx}(L,t) = U_2(t),\\ \Upsilon(0,t) = \Upsilon_x(0,t) = 0,\\ \Upsilon(x,0) = \Upsilon_0(x), \Upsilon_t(x,0) = \Upsilon_1(x),\end{cases} \tag{5}$$

for all $x \in (0, L)$ and $t \geq 0$, where Υ_0 represents the initial displacement of the flexible marine riser, Υ_1 denotes the initial velocity, and $U_1(t)$ and $U_2(t)$ are the boundary control force and torque, respectively, applied at the top boundary of the marine riser, as depicted in Fig. 1. It's worth mentioning that linear boundary controls have often been used in the literature to ensure stability for the various specialized types of beams mentioned earlier. Nevertheless, when it comes to handling saturation phenomena, dealing with large deformations, or employing intelligent materials in practical engineering scenarios, nonlinear boundary control gains significance. This is because the controller must accommodate the nonlinear behavior exhibited by sensors and actuators.

This motivates us to consider the following nonlinear boundary feedback controls:

$$\begin{cases}U_1(t) = -F_1(\Upsilon_t(L,t)),\\ U_2(t) = -F_2(\Upsilon_{xt}(L,t)),\end{cases} \tag{6}$$

where $\Upsilon_t(L,t)$ and $\Upsilon_{xt}(L,t)$ represent respectively the measured velocity and angular velocity at the top end of the marine riser. The functions $F_i(\cdot), i = 1, 2$ are monotonic non-decreasing and continuous, satisfying

$$F_i(0) = 0 \text{ and } F_i(\tau)\tau > 0, \ \forall\tau \neq 0, \tag{7a}$$

$$a \leq \frac{F_i(\tau)}{\tau} \leq b, \quad \forall|\tau| \geq \mu, \tag{7b}$$

for given constants $b \geq a > 0$ and $\mu > 0$. In general terms, the nonlinear boundary controls described by (6) serve a similar function to that of linear negative feedback of velocity and angular velocity, based on the passivity principle, to generate a dissipation effect. This aligns with the observation that negative velocity feedback aids in increasing damping in most infinite-dimensional inertial systems, such as large flexible structures and fluid-conveying pipeline systems.

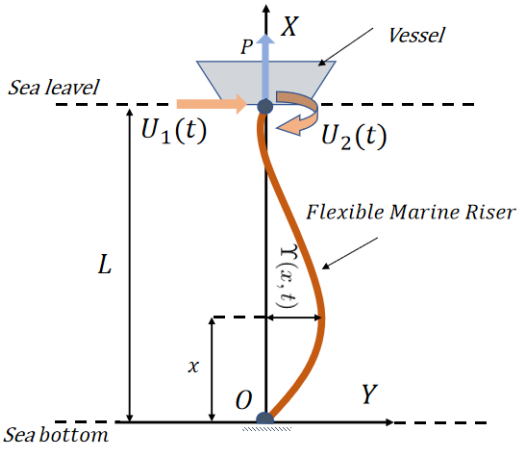

Fig. 1. Schematic representation of a flexible marine riser under two boundary controls.

B. System modeling

The nonlinear flexible marine riser system is depicted in Fig. 1, where the top end of the riser is attached to the vessel while the bottom end remains fixed. P denotes the initial tension at the top of the riser, and the control inputs $U_1(t)$ and $U_2(t)$ are exerted at the top boundary of the riser. The kinetic energy $\mathcal{K}$ of this flexible marine riser system can be expressed as

$$\mathcal{K}(t) = \frac{\rho I}{2}\int_0^L \Upsilon_{xt}^2(x,t)dx + \frac{\rho\Lambda}{2}\int_0^L \Upsilon_t^2(x,t)dx, \tag{8}$$

where ρI and $\rho\Lambda$ are defined in (1) and L represents the length of the marine riser. The potential energy $\mathcal{U}$ can be expressed by

$$\begin{aligned}\mathcal{U}(t) \ = \ & P\int_0^L \mathscr{E}(x,t)dx + \frac{E\Lambda}{2}\int_0^L [\mathscr{E}(x,t)]^2dx\\ &+\frac{EI}{2}\int_0^L \Upsilon_{xx}^2(x,t)dx,\end{aligned} \tag{9}$$

where $\mathscr{E}(x,t) = (1+\Upsilon_x^2(x,t))^{\frac{1}{2}} - 1$ signifies the geometric strain relationship elaborated in [27], [28]; while $\mathcal{E}\Lambda$ and EI are interpreted in (1). In (9), the first term arises from tension, the second term represents strain potential energy, and the third term reflects the bending moment. The work exerted by the translational boundary actuator is given by

$$W_{c1} = U_1(t)\Upsilon(L,t).$$

The work exerted by the torque is given by

$$W_{c2} = U_2(t)[\Upsilon_x(L,t)].$$

The total work applied on the system is given by

$$W_c = W_{c1} + W_{c2} = U_1(t)\Upsilon(L,t) + U_2(t)\Upsilon_x(L,t). \tag{10}$$

Hamilton's principle [36] in variational form states that

$$\int_{t_0}^{t_1} (\delta\mathcal{K} - \delta\mathcal{U} + \delta W_c)dt = 0, \tag{11}$$

where δ denotes the variational operator, and can then be applied to derive the system model (1) and boundary conditions (5) of the flexible marine riser. The details is put as Appendix.

C. The work of this paper

As previously mentioned, the primary focus of this paper is to establish boundary stabilization and decay rate estimation for the nonlinear flexible marine riser systems described by (1) and (5), under the nonlinear controls (6).

To achieve this objective, we encounter two significant challenges. Firstly, we need to address the well-posedness of the closed-loop system (1) subject to the nonlinear boundary controls (6). This closed-loop system exhibits substantial nonlinearity, arising both from the inherent nonlinearity of the system and from the nonlinear controls themselves. As a result, commonly used approaches such as the semigroup of contractions [43], the Faedo-Galerkin method [16], the linear C_0-semigroup with Lipschitz perturbation method [17], and the fixed point theorem [9] are not applicable in this context.

Secondly, the stability analysis of the nonlinear flexible system considered in this paper poses significant difficulties. Many commonly used methods for analyzing the stability of nonlinear flexible systems, including the Lyapunov method [33], the frequency domain method [29], the energy perturbation method [8], the integral multiplier method [24], and the approximately observable method [38], are not suitable due to the combined effects of rotational inertia, system nonlinearity, and nonlinear boundary controls. These factors introduce major technical complexities that hinder the stability analysis of the system.

Another challenge lies in determining the decay rate of the solution and the energy. Since Lasiecka's work [30] introduced an estimation method for the decay rate of wave equations, numerous related studies have been conducted. These include investigations into wave equations [6], [32], nonlinear dissipative hyperbolic systems [2], infinite-dimensional vibrating damped systems [3], beam equations [1], [5], and the von Karman system with internal damping [23].

A notable contribution was made in [32], where a method for constructing explicit energy decay rates was presented. It's worth mentioning that optimal decay rates, partially considered in [4], were fully addressed in [2] by selecting an optimal weight function. However, applying these methods to multiple nonlinear boundary control problems involving nonlinear partial differential equations (PDEs) is challenging. This difficulty arises from the complexity of finding appropriate multipliers.

D. Contributions of the paper

This paper makes several contributions. Firstly, we derive a nonlinear system model for the flexible marine riser that incorporates the rotational inertia term. This model provides a more accurate representation of larger amplitude vibrations compared to the models presented in [14], [18], [33], and [42]. To address the complexities arising from rotational inertia, nonlinear tension, and nonlinear controls, we employ nonlinear semigroup theory to establish the well-posedness of the closed-loop system.

Secondly, the paper introduces two nonlinear boundary feedback controls that satisfy conditions (7a) and (7b), encompassing a broad range of nonlinear feedback laws. Since $F_i(\cdot), i = 1, 2$ are not specifically defined near the origin and are not required to be strictly monotonically increasing over $\mathbb{R}$, they cover conditions like the slope-sector condition [10], [26], [35] and the slope-restricted condition [12], [25], among others.

Thirdly, the inclusion of rotational inertia poses challenges in finding an appropriate energy perturbation or integral multiplier for stability analysis of the closed-loop system. To overcome this, we introduce a novel method where the existence interval of the integral multiplier is determined through an adjustment term. Drawing inspiration from [30], the solutions and energy function of the closed-loop system are governed by the solution of a dissipative ordinary differential equation (ODE):

$$\frac{\mathrm{d}}{\mathrm{d}t}\mathcal{S}(t) + \Psi(\mathcal{S}(t)) = 0, \quad t > 0, \tag{12}$$

where the function $\Psi(\cdot)$ relies on a newly introduced average concave function that is closely related to the nonlinear feedbacks F_i. In brief, the asymptotic stability of the closed-loop system can be inferred. Finally, if the behavior of F_i near zero is known, the decay rate of the closed-loop system can be approximated by solving ODE (12). When F_i are monotonic non-decreasing functions (locally saturated) in the vicinity of zero, a novel approach for estimating the decay rate has been devised. By further categorizing the nonlinear feedbacks, we can obtain three primary types of decay patterns, which are supported by numerical simulations of three distinct sets of examples.

E. Organizations

In the subsequent section, Section II, the well-posedness of the closed-loop system is established through the application of nonlinear semigroup theory. The asymptotic stability of this system is then proven in Section III by solving a dissipative ODE, and further estimating the decay behaviors of both the

energy and the solution within the closed-loop system. To illustrate these theoretical findings, Section IV presents a series of numerical simulations. Finally, Section V concludes the paper, summarizing the key results. For those interested in the model's derivation, it is detailed in the Appendix.

F. Notations

Throughout this paper, let $\langle\cdot,\cdot\rangle$ denote the inner product in $\mathcal{L}^2(0,L)$ with the inner product induced norm $\|\cdot\|$. Furthermore, we introduce two closed subspaces

$$V := \{\Upsilon \in H^1(0,L) | \Upsilon(0) = 0\},$$
$$W := \{\Upsilon \in H^2(0,L) | \Upsilon(0) = \Upsilon_x(0) = 0\}.$$

It is straightforward to observe that $W \subset V \subset \mathcal{L}^2(0,L) \subset V' \subset W'$, where W' and V' represent the dual spaces of W and V, respectively. The norms on V and W are defined as follows:

$$\|\Upsilon\|_V^2 := \int_0^L [\rho\Lambda\Upsilon^2(x,t) + \rho I\Upsilon_x^2(x,t)]dx, \ \forall \Upsilon \in V, \quad (13a)$$

$$\|\Upsilon\|_W^2 := \mathcal{E}I \int_0^L \Upsilon_{xx}^2(x,t)dx, \ \forall \Upsilon \in W. \quad (13b)$$

Define the state space as $H_e^3 = H^3(0,L) \cap W$ and $H = W \times V$ equipped with the norm $\|(f,g)^\top\|_H^2 = \|f\|_W^2 + \|g\|_V^2$ for any $(f,g)^\top \in H$.

II. Well-posedness of closed-loop system

To apply the nonlinear semigroup theory, we firstly formulate the system in an abstract form. The closed-loop of our system now reads as follows:

$$\rho\Lambda\Upsilon_{tt}(x,t) - \rho I\Upsilon_{xxtt}(x,t) + \mathcal{E}I\Upsilon_{xxxx}(x,t) = \Big[(\mathcal{E}\Lambda + \frac{P-\mathcal{E}\Lambda}{\sqrt{1+\Upsilon_x^2(x,t)}})\Upsilon_x(x,t)\Big]_x, \quad (14a)$$

$$\rho I\Upsilon_{xtt}(L,t) + (\mathcal{E}\Lambda + \frac{P-\mathcal{E}\Lambda}{\sqrt{1+\Upsilon_x^2(L,t)}})\Upsilon_x(L,t) - \mathcal{E}I\Upsilon_{xxx}(L,t) = -F_1(\Upsilon_t(L,t)), \quad (14b)$$

$$\mathcal{E}I\Upsilon_{xx}(L,t) = -F_2(\Upsilon_{xt}(L,t)), \quad (14c)$$

$$\Upsilon(0,t) = \Upsilon_x(0,t) = 0, \quad (14d)$$

$$\Upsilon(x,0) = \Upsilon_0(x), \Upsilon_t(x,0) = \Upsilon_1(x), \quad (14e)$$

for all $x \in (0,L)$ and any $t \geq 0$. From a physical perspective, the initial tension is typically much smaller than the tensile stiffness, that is to say, $P \leq \mathcal{E}\Lambda$, as discussed in [28], [41]. The energy function of the closed-loop system (14a)-(14e) is defined by

$$\mathbb{E}(t) := \frac{1}{2}\int_0^L [\mathcal{E}I\Upsilon_{xx}^2(x,t) + \rho\Lambda\Upsilon_t^2(x,t) + \rho I\Upsilon_{xt}^2(x,t)]dx + \frac{1}{2}\int_0^L \int_0^{\Upsilon_x^2(x,t)} \big(\mathcal{E}\Lambda + \frac{P-\mathcal{E}\Lambda}{\sqrt{1+\theta}}\big)d\theta dx \quad (15)$$

Remark II.1. *The nonlinear feedback functions are presumed to be monotonic non-decreasing and continuous, an assumption that has been utilized in [11], [32]. Furthermore, these functions are, in reality, also monotonically increasing and continuous, a property that has been exploited in various works such as [2], [5], [30], [31].*

For notational simplicity and clarity, we shall omit the obvious variables x and t hereafter. Now, we aim to establish the well-posedness of the closed-loop system (14a)-(14e) through the application of the nonlinear semigroup theory, specifically referencing [13, Theorem 7.2].

Multiplying both sides of equation (14a) by $u \in W$ and integrating by parts from 0 to L, we derive the variational structure corresponding to the closed-loop system (14a)-(14e). This variational structure is given by:

$$\rho\Lambda\int_0^L \Upsilon_{tt}udx + \rho I\int_0^L \Upsilon_{xtt}u_x dx + \mathcal{E}I\int_0^L \Upsilon_{xx}u_{xx}dx + F_1(\Upsilon_t(L,t))u(L) + F_2(\Upsilon_{xt}(L,t))u_x(L) + \int_0^L (\mathcal{E}\Lambda + \frac{P-\mathcal{E}\Lambda}{\sqrt{1+\Upsilon_x^2}})\Upsilon_x u_x dx = 0, \quad \forall u \in W. \quad (16)$$

Based on equation (16), we now introduce two linear operators as follows: $\mathcal{A}: V \to V'$ and $\mathcal{B}: W \to W'$ by

$$\langle \mathcal{A}f, g\rangle_{V',V} := \langle f,g\rangle_V = \int_0^L [\rho\Lambda fg + \rho I f_x g_x]dx, \forall f,g \in V,$$
$$\langle \mathcal{B}f, g\rangle_{W',W} := \langle f,g\rangle_W = \mathcal{E}I\int_0^L f_{xx}g_{xx}dx, \forall f,g \in W,$$

and the nonlinear operators $D: V \to V'$ and $D_1,\ \mathcal{T}: W \to W'$ given by

$$\langle Df, g\rangle_{V',V} := F_1(f(L))g(L), \quad \forall f,g \in V,$$
$$\langle D_1 f, g\rangle_{W',W} := F_2(f_x(L))g_x(L), \quad \forall f,g \in W,$$
$$\langle \mathcal{T}f, g\rangle_{W',W} := \int_0^L f_x(\mathcal{E}\Lambda + \frac{P-\mathcal{E}\Lambda}{\sqrt{1+f_x^2}})g_x dx, \forall f,g \in W.$$

Then, the equation (16) can be equivalently expressed as

$$\langle \mathcal{A}\Upsilon_{tt} + \mathcal{B}\Upsilon + \mathcal{T}\Upsilon + D\Upsilon_t + D_1\Upsilon_t, u\rangle_{W',W} = 0, \forall u \in W.$$

As a result,

$$\mathcal{A}\Upsilon_{tt} + \mathcal{B}\Upsilon + \mathcal{T}\Upsilon + D\Upsilon_t + D_1\Upsilon_t = 0 \text{ in } W', \quad (17)$$

which corresponds to the weak solution of the closed-loop system (14a)-(14e). It is straightforward to verify that $\mathcal{A}: V \to V'$ is an isomorphic mapping. Consequently, (17) can be reformulated as

$$\begin{pmatrix}\Upsilon\\ \Upsilon_t\end{pmatrix}_t + \begin{pmatrix}0 & -\mathcal{I}\\ \mathcal{A}^{-1}\mathcal{B} & \mathcal{A}^{-1}D + \mathcal{A}^{-1}D_1\end{pmatrix}\begin{pmatrix}\Upsilon\\ \Upsilon_t\end{pmatrix} = \begin{pmatrix}0 & 0\\ -\mathcal{A}^{-1}\mathcal{T} & 0\end{pmatrix}\begin{pmatrix}\Upsilon\\ \Upsilon_t\end{pmatrix}. \quad (18)$$

Equation (18) can be further simplified to

$$M_t + \mathfrak{A}M = \mathfrak{G}M, \quad (19)$$

where $M := (\Upsilon, \Upsilon_t)^\top$, the nonlinear operator $\mathfrak{A}: \mathcal{D}(\mathfrak{A}) \subset H \to H$ defined by

$$\mathfrak{A}M = \mathfrak{A}\begin{pmatrix}f\\ g\end{pmatrix} = \begin{pmatrix}-g\\ \mathcal{A}^{-1}(\mathcal{B}f + Dg + D_1 g)\end{pmatrix}, \quad (20)$$

for any $(f,g)^\top \in \mathcal{D}(\mathfrak{A})$:

$$\mathcal{D}(\mathfrak{A}) = \{(f,g)^\top \in W \times W | \mathcal{B}f + Dg + D_1 g \in V'\}, \quad (21)$$

and the operator $\mathfrak{G} : H \to H$ is defined by

$$\mathfrak{G}M = \mathfrak{G}\begin{pmatrix} f \\ g \end{pmatrix} = \begin{pmatrix} 0 \\ -\mathcal{A}^{-1}\mathcal{T}f \end{pmatrix}, \quad (22)$$

for any $(f,g)^\top \in H$.

Proposition II.1 below provides an exact description of $\mathcal{D}(\mathfrak{A})$.

Proposition II.1. *The set $\mathcal{D}(\mathfrak{A})$ is composed of pairs $(f,g)^\top \in H_e^3 \times W$ satisfying the boundary condition $\mathcal{E}If_{xx}(L) = -F_2(g_x(L))$.*

Proof: From definition (20), it is evident that $(f,g)^\top \in \mathcal{D}(\mathfrak{A})$ if and only if $f, g \in W$ such that

$$\mathcal{E}I\langle f_{xx}, u_{xx}\rangle + F_1(g(L))u(L) + F_2(g_x(L))u_x(L) = \langle \breve{a}, u\rangle_{V',V} \quad (23)$$

for any $u \in W$ and some $\breve{a} \in V'$, which can be simplified as

$$\mathcal{E}I\langle f_{xx}, u_{xx}\rangle + F_2(g_x(L))u_x(L) = \langle \Pi, u\rangle_{V',V}, \quad (24)$$

for any $u \in W$, where $\Pi = -Dg + \breve{a}$. If $f \in H^3(0,L)$. Letting $u \in H_0^2 := \{u \in W : u_x(L) = 0\}$ in (24) gives

$$\mathcal{E}I\langle f_{xxx}, u_x\rangle = -\langle \Pi, u\rangle_{V',V}. \quad (25)$$

Carrying out integration by parts in (24) yields

$$\mathcal{E}I\langle f_{xxx}, u_x\rangle - (F_2(g_x(L)) + \mathcal{E}If_{xx}(L))u_x(L) = -\langle \Pi, u\rangle_{V',V},$$

for any $u \in W$, which, together with (25), yields $\mathcal{E}If_{xx}(L) = -F_2(g_x(L))$.

Next, it suffices to prove that $f \in H^3(0,L)$. Set $\overline{f} = \lambda_1 x^2 + \lambda_2 x^3$ with $\lambda_1 = \frac{LF_1(g(L)) + F_2(g_x(L))}{-2\mathcal{E}I}$, and $\lambda_2 = \frac{F_1(g(L))}{6\mathcal{E}I}$. It is then straightforward to verify that

$$-\mathcal{E}I\langle \overline{f}_{xx}, u_{xx}\rangle = F_1(g(L))u(L) + F_2(g_x(L))u_x(L).$$

Therefore, the equation (23) is equivalent to $\mathcal{B}(f - \overline{f}) = \breve{a}$. We now proceed to demonstrate that $\widehat{f} = f - \overline{f} \in H^3(0,L)$ using interpolation. By the elliptic operator theory, the problem $\mathcal{B}\widehat{f} = \breve{a}$ possesses a unique solution $\widehat{f} \in W$ if $\breve{a} \in W'$. This establishes a linear and continuous mapping $\breve{a} \to \widehat{f} : W' \to W$. Furthermore, if $\breve{a} \in \mathcal{L}^2(0,L)$, the problem $\mathcal{B}\widehat{f} = \breve{a}$ admits a unique solution $\widehat{f} \in H^4(0,L)$. This defines a linear and continuous mapping $\breve{a} \to \widehat{f} : \mathcal{L}^2(0,L) \to H^4(0,L)$. Employing interpolation, we deduce that if $\breve{a} \in V'$, then $\widehat{f} \in H^3(0,L)$. Since $f = \widehat{f} + \overline{f}$, this implies that $f \in H_e^3$. ∎

A. Proof of well-posedness

Lemmas II.1 and II.2 play a crucial role in establishing the well-posedness of the closed-loop system through the application of the nonlinear semigroup theory.

Lemma II.1. *The operator $\mathfrak{A}$ is an maximal monotone operator in H.*

Proof: For any $M_1 = (f,g)^\top, M_2 = (\tilde{f},\tilde{g})^\top \in \mathcal{D}(\mathfrak{A})$, from (20), we have

$$\begin{aligned}
&\langle \mathfrak{A}M_1 - \mathfrak{A}M_2, M_1 - M_2\rangle_H \\
&= \langle \mathcal{B}(f-\tilde{f}), g-\tilde{g}\rangle_{W',W} + \langle Dg - D\tilde{g}, g-\tilde{g}\rangle_{V',V} \\
&\quad + \langle D_1 g - D_1\tilde{g}, g-\tilde{g}\rangle_{W',W} - \langle f-\tilde{f}, g-\tilde{g}\rangle_W \\
&= [F_1(g(L)) - F_1(\tilde{g}(L))](g(L) - \tilde{g}(L)) \\
&\quad + [F_2(g_x(L)) - F_2(\tilde{g}_x(L))](g_x(L) - \tilde{g}_x(L)). \quad (26)
\end{aligned}$$

Since $F_i(\cdot), i = 1,2$, are monotonic non-decreasing and continuous functions over $\mathbb{R}$, it follows that

$$\begin{aligned}
&[F_2(g_x(L)) - F_2(\tilde{g}_x(L))](g_x(L) - \tilde{g}_x(L)) \\
&+[F_1(g(L)) - F_1(\tilde{g}(L))](g(L) - \tilde{g}(L)) \geq 0, \quad (27)
\end{aligned}$$

which, together with (26), leads to

$$\langle \mathfrak{A}M_1 - \mathfrak{A}M_2, M_1 - M_2\rangle_H \geq 0. \quad (28)$$

Therefore, the operator $\mathfrak{A}$ is monotone.

In what follows, we aim to prove that the operator $\mathfrak{I} + \mathfrak{A}$ is surjective, where $\mathfrak{I}$ denotes the identity mapping on H. This proof is equivalent to demonstrating that the mapping $\mathcal{I} + \mathcal{A}^{-1}(\mathcal{B} + D + D_1) : W \to W'$ is onto, with $\mathcal{I}$ representing the identity mapping on W. Indeed, if $\mathcal{I} + \mathcal{A}^{-1}(\mathcal{B} + D + D_1)$ is onto, then for any given $(x_1, x_2)^\top \in H$, there exists a $g \in W$ such that $(\mathcal{A} + \mathcal{B} + D + D_1)g = \mathcal{A}x_2 - \mathcal{B}x_1$. Clearly, by letting $f = x_1 + g$, we obtain $(f,g)^\top \in W \times W$. Furthermore, we have

$$\mathcal{A}^{-1}(\mathcal{B}f + Dg + D_1 g) = \mathcal{A}^{-1}(\mathcal{B}g + \mathcal{B}x_1 + Dg + D_1 g) = x_2 - g \in V,$$

which implies that $(f,g)^\top \in \mathcal{D}(\mathfrak{A})$. In order to

$$(\mathfrak{I} + \mathfrak{A})\begin{pmatrix} f \\ g \end{pmatrix} = \begin{pmatrix} x_1 \\ x_2 \end{pmatrix},$$

it is necessary to demonstrate the surjectivity of $\mathcal{A} + \mathcal{B} + D + D_1$. To accomplish this, let us fix $x_2 \in V'$, and introduce the variational function $\mathcal{F}(g) : W \to \mathbb{R}$ defined as

$$\mathcal{F}(g) := \frac{1}{2}\|g\|_V^2 + \frac{1}{2}\|g\|_W^2 + G(g) + Z(g_x) - \langle x_2, g\rangle_{W',W}, \quad (29)$$

where $g \in W$ and the maps $G : V \to \mathbb{R}$ and $Z : W \to \mathbb{R}$ are given by

$$G(g) = \int_0^{g(L)} F_1(\varrho)d\varrho, \ Z(g_x) = \int_0^{g_x(L)} F_2(\vartheta)d\vartheta. \quad (30)$$

Since $F_i(\cdot), i = 1,2$ are continuous and monotonic non-decreasing functions, it follows that the function $\mathcal{F}$ is well-defined and continuously differentiable, and

$$\langle \mathcal{F}'(g), v\rangle_{W',W} = \langle (\mathcal{A} + \mathcal{B} + D + D_1)g - x_2, v\rangle_{W',W}, \forall g, v \in W.$$

By the condition (7a) and the definition (30), we can determine that $G(g) \geq 0$ and $Z(g_x) \geq 0$. Consequently, it follows from (29) that

$$\mathcal{F}(g) \geq C\big[\frac{1}{2}\|g\|_W - \|x_2\|_{W'}\big]\|g\|_W, \quad (31)$$

with some positive constant C. This implies that as $\|g\|_W \to \infty$, $\mathcal{F}(g) \to +\infty$, i.e., $\mathcal{F}$ is coercive. Consequently, in light of Theorem 1.1 from [44, p.4], it is evident that the infimum of

$\mathcal{F}$ is attained at a specific point $g \in W$. Therefore, we have $\mathcal{F}'(g) = 0$, which is equivalent to $(\mathcal{A}+\mathcal{B}+D+D_1)g = x_2$ in W'. This establishes the maximal monotonicity of $\mathfrak{A}$. ■

Lemma II.2. *$\mathfrak{G}$ is locally Lipschitz on H.*

Proof: Set

$$h(\tau) := \mathcal{E}\Lambda\tau + \frac{(P-\mathcal{E}\Lambda)\tau}{\sqrt{1+\tau^2}}, P \le \mathcal{E}\Lambda, \forall \tau \in \mathbb{R}.$$

It is straightforward to observe that

$$P \le \frac{\mathrm{d}h(\tau)}{\mathrm{d}\tau} < \mathcal{E}\Lambda, \ \forall \tau \in \mathbb{R}.$$

Furthermore, we can ascertain that $h(\cdot)$ is a monotonic increasing function on $\mathbb{R}$ which fulfills the following condition:

$$\big|h(\tau_1) - h(\tau_2)\big| < \mathcal{E}\Lambda|\tau_1 - \tau_2|, \quad \forall \tau_1, \tau_2 \in \mathbb{R}. \tag{32}$$

Therefore, for any $M_1 = (f,g)^\top, M_2 = (\tilde{f},\tilde{g})^\top \in \mathcal{D}(\mathfrak{A})$, we can infer from equations (22) and (32) that

$$\begin{aligned}
&\big|\langle \mathfrak{G}M_1 - \mathfrak{G}M_2, M_1 - M_2\rangle_H\big| \\
&= \left|\left\langle \begin{pmatrix} 0 \\ -\mathcal{A}^{-1}\mathcal{T}f + \mathcal{A}^{-1}\mathcal{T}\tilde{f}\end{pmatrix}, \begin{pmatrix} f-\tilde{f} \\ g-\tilde{g}\end{pmatrix}\right\rangle_H\right| \\
&= \left|\int_0^L \Big[f_x(\mathcal{E}\Lambda + \frac{P-\mathcal{E}\Lambda}{\sqrt{1+f_x^2}}) - \tilde{f}_x(\mathcal{E}\Lambda + \frac{P-\mathcal{E}\Lambda}{\sqrt{1+\tilde{f}_x^2}})\Big](g_x - \tilde{g}_x)dx\right| \\
&= \left|\int_0^L [h(f_x) - h(\tilde{f}_x)](g_x - \tilde{g}_x)dx\right| \\
&\le \frac{\mathcal{E}\Lambda}{2}\int_0^L [(f_x - \tilde{f}_x)^2 + (g_x - \tilde{g}_x)^2]dx \\
&\le \frac{\mathcal{E}\Lambda L}{2}\int_0^L (f_{xx} - \tilde{f}_{xx})^2 dx + \frac{\mathcal{E}\Lambda}{2}\int_0^L [(g_x - \tilde{g}_x)^2 + (g - \tilde{g})^2]dx \\
&\le \kappa \|M_1 - M_2\|_H^2,
\end{aligned} \tag{33}$$

where $\kappa = \max\{\frac{\Lambda L}{2I}, \frac{\mathcal{E}\Lambda}{2\rho I}\}$ and Poincaré inequality ($\|y_x\|^2 \le L\|y_{xx}\|^2$) was used. ■

Lemma II.3 following implies that the energy $\mathbb{E}(t)$ is monotonic non-increasing.

Lemma II.3. *Assume that $\Upsilon(\cdot,\cdot)$ is a strong solution of the closed-loop system (14a)-(14e). Then,*

$$\frac{\mathrm{d}}{\mathrm{d}t}\mathbb{E}(t) = -F_1(\Upsilon_t(L,t))\Upsilon_t(L,t) - F_2(\Upsilon_{xt}(L,t))\Upsilon_{xt}(L,t), \tag{34}$$

which means, based on the condition (7a), that $E(t)$ is monotonic non-increasing. In other words, $E(t) \le E(0)$ for all $t \ge 0$.

Proof: From the definition (15), one obtains

$$\begin{aligned}
\frac{\mathrm{d}\mathbb{E}(t)}{\mathrm{d}t} &= \rho\Lambda\int_0^L \Upsilon_t\Upsilon_{tt}dx + \rho I\int_0^L \Upsilon_{xt}\Upsilon_{xtt}dx \\
&+ \mathcal{E}I\int_0^L \Upsilon_{xx}\Upsilon_{xxt}dx + \int_0^L (\mathcal{E}\Lambda + \frac{P-\mathcal{E}\Lambda}{\sqrt{1+\Upsilon_x^2}})\Upsilon_x\Upsilon_{xt}dx,
\end{aligned} \tag{35}$$

which, together with the integration by parts, gives

$$\begin{aligned}
\frac{\mathrm{d}\mathbb{E}(t)}{\mathrm{d}t} =& \rho\Lambda\int_0^L \Upsilon_{tt}\Upsilon_t dx - \mathcal{E}I\int_0^L \Upsilon_{xxx}\Upsilon_{xt}dx - \rho I\int_0^L \Upsilon_{xxtt}\Upsilon_t dx \\
&+ \mathcal{E}I\Upsilon_{xx}(L,t)\Upsilon_{xt}(L,t) - \int_0^L \Big[(\mathcal{E}\Lambda + \frac{P-\mathcal{E}\Lambda}{\sqrt{1+\Upsilon_x^2}})\Upsilon_x\Big]_x\Upsilon_t dx \\
&+ \Big[(\mathcal{E}\Lambda + \frac{P-\mathcal{E}\Lambda}{\sqrt{1+\Upsilon_x^2(L,t)}})\Upsilon_x(L,t) + \rho I\Upsilon_{xtt}(L,t)\Big]\Upsilon_t(L,t) \\
=& -\mathcal{E}I\Upsilon_{xxx}(L,t)\Upsilon_t(L,t) + \rho I\Upsilon_{xtt}(L,t)\Upsilon_t(L,t) \\
&+ \int_0^L (\rho\Lambda\Upsilon_{tt} - \rho I\Upsilon_{xxtt} + \mathcal{E}I\Upsilon_{xxxx})\Upsilon_t dt \\
&+ (\mathcal{E}\Lambda + \frac{P-\mathcal{E}\Lambda}{\sqrt{1+\Upsilon_x^2(L,t)}})\Upsilon_x(L,t)\Upsilon_t(L,t) \\
&- \int_0^L \Big[(\mathcal{E}\Lambda + \frac{P-\mathcal{E}\Lambda}{\sqrt{1+\Upsilon_x^2}})\Upsilon_x\Big]_x\Upsilon_t dx \\
&+ \mathcal{E}I\Upsilon_{xx}(L,t)\Upsilon_{xt}(L,t).
\end{aligned} \tag{36}$$

The desired result is then obtained by applying (14a), (14b), and (14c). ■

Using the nonlinear semigroup theory, one can define strong solutions to the system (14a)-(14e) where the initial data belongs to the domain of the generator. Additionally, weak solutions can be regarded as limits of strong solutions for almost everywhere in t, as referenced in [13].

Theorem II.1. *Suppose the condition (7a) and the initial data $M_0 := (\Upsilon_0, \Upsilon_1)^\top \in \mathcal{D}(\mathfrak{A})$. Then there exists a unique strong solution $M = (\Upsilon, \Upsilon_t)^\top \in \mathcal{W}^{1,\infty}(0,\infty;\mathcal{D}(\mathfrak{A}))$ for the evolution equation (19), i.e., the closed-loop system (14a)-(14e) admits a unique strong solution $\Upsilon(\cdot,\cdot)$ such that*

$$\Upsilon \in \mathcal{W}^{2,\infty}(0,\infty;W) \cap \mathcal{W}^{1,\infty}(0,\infty;H_e^3). \tag{37}$$

If the initial data $M_0 := (\Upsilon_0, \Upsilon_1)^\top \in H$, then there exists a unique weak solution $M = (\Upsilon, \Upsilon_t)^\top \in C(0,\infty;H)$ for the evolution equation (19), i.e., the closed-loop system (14a)-(14e) admits a unique weak solution $\Upsilon(\cdot,\cdot)$ such that

$$\Upsilon \in C(0,\infty;W) \cap C^1(0,\infty;V), \tag{38}$$

which depends continuously on the initial data $(\Upsilon_0, \Upsilon_1)^\top$ in H.

Proof: Thanks to Lemmas II.1 and II.2, it has been established that $\mathfrak{A}$ is maximal monotone and $\mathfrak{G}$ is Lipschitz on H. By invoking [13, Theorem 7.2], we can deduce that there exists $t_m \le \infty$ such that for all $M_0 = (\Upsilon_0, \Upsilon_1)^\top \in \mathcal{D}(\mathfrak{A})$, there exists a unique strong solution $M = (\Upsilon, \Upsilon_t)^\top \in \mathcal{W}^{1,\infty}(0,t_m;\mathcal{D}(\mathfrak{A}))$ to the evolution equation (19). This result, combined with Proposition II.1, leads to the conclusion that

$$(\Upsilon, \Upsilon_t)^\top \in \mathcal{W}^{1,\infty}(0,\infty;H_e^3 \times W).$$

Furthermore, if $t_m < \infty$, then $\limsup_{t\to t_m^-} \|M\|_H = \infty$. This assertion follows from the fact that the energy function $E(t)$ is monotonic non-increasing, as stated in Lemma II.3. Specifically, we have $\mathbb{E}(t) \le \mathbb{E}(0)$ for all $t \in (0,t_m)$. Combining this with (13a) and (13b), we obtain

$$\|M\|_H^2 = \|\Upsilon\|_W^2 + \|\Upsilon_t\|_V^2 \le 2\mathbb{E}(t) \le 2\mathbb{E}(0). \tag{39}$$

This leads to a contradiction, specifically, the assumption that $t_m < \infty$ cannot hold. Therefore, we conclude that $t_m = \infty$, which implies that the strong solution is globally defined.

Let $M_1 = (f, g)^\top, M_2 = (\tilde{f}, \tilde{g})^\top \in \mathcal{D}(\mathfrak{A})$ be two strong solutions of (19) with initial value $M_1(0)$ and $M_2(0)$, respectively. From (19), we have

$$\left(\frac{\mathrm{d}M_1}{\mathrm{d}t} - \frac{\mathrm{d}M_2}{\mathrm{d}t}\right) + \mathfrak{A}(M_1 - M_2) = \mathfrak{G}(M_1) - \mathfrak{G}(M_2). \quad (40)$$

Taking the inner product of both sides of (40) with $M_1 - M_2$ and integrating from 0 to t, we derive the following expression:

$$\begin{aligned} &\|M_1 - M_2\|_H^2 - \|M_1(0) - M_2(0)\|_H^2 \\ &\quad + \int_0^t \langle \mathfrak{A}(M_1 - M_2), M_1 - M_2\rangle_H ds \\ &= \int_0^t \langle \mathfrak{G}(M_1) - \mathfrak{G}(M_2), M_1 - M_2\rangle_H ds. \end{aligned} \quad (41)$$

It follows from Lemma II.1 and (41) that

$$\begin{aligned} \|M_1 - M_2\|_H^2 \le \int_0^t \langle \mathfrak{G}M_1 - \mathfrak{G}M_2, M_1 - M_2\rangle_H ds \\ + \|M_1(0) - M_2(0)\|_H^2. \end{aligned} \quad (42)$$

Invoking Lemma II.2 and equation (42), we derive

$$\|M_1 - M_2\|_H^2 \le \kappa \int_0^t \|M_1 - M_2\|_H^2 ds + \|M_1(0) - M_2(0)\|_H^2,$$

with the constant κ given in (33). From Gronwall's inequality, it follows that

$$\|M_1 - M_2\|_H^2 \le e^{\kappa t}\|M_1(0) - M_2(0)\|_H^2, \quad \forall t \in [0, T]. \quad (43)$$

This means the strong solution depends continuously on the initial value in H. Since $\mathcal{D}(\mathfrak{A})$ is dense in H, (43) means that for any $M_0 = (\Upsilon_0, \Upsilon_1)^\top \in H$, there exists a unique weak solution $M = (\Upsilon, \Upsilon_t)^\top \in C(0, \infty; H)$ to the evolution equation (19). This is equivalent in turn to the existence of the weak solution of the closed-loop system (14a)-(14e). Moreover, the weak solution also depends continuously on the initial value in H.

■

III. Stability of Closed-Loop System

A. Stability analysis

In this section, we aim to establish the stability of the closed-loop system (14a)-(14e). We achieve this by adopting an approach introduced in [30]. To proceed, we first introduce several definitions and preliminary results that are crucial for our analysis.

For $i = 1, 2$, let us assume the existence of maps $\mathfrak{W}_i(\tau)$ that are monotonic strictly increasing and concave for $\tau \ge 0$ with the property $\mathfrak{W}_i(0) = 0$. These maps satisfy the given conditions:

$$\mathfrak{W}_i(\tau F_i(\tau)) \ge \tau^2 + [F_i(\tau)]^2, \ i = 1, 2, \quad \forall |\tau| \le \mu, \quad (44)$$

where μ is is the constant specified in (7b). Based on the distinct decay behaviors of the nonlinear feedbacks F_i near zero, it becomes evident that the function $\mathfrak{W}_i$ can be readily identified to fulfill (44). This assertion will be exemplified through several cases presented in subsection III-B later on. Now, let us define

$$\hat{\mathfrak{W}}_i(\tau) = \mathfrak{W}_i\left(\frac{\tau}{T}\right), \ i = 1, 2, \quad \forall \tau \in \mathbb{R}, \quad (45)$$

where T is a constant determined later. Given a constant $\sigma > 0$ and denoting $\mathcal{I}$ as the identity mapping, it is straightforward to observe that $\sigma\mathcal{I} + \frac{\hat{\mathfrak{W}}_1 + \hat{\mathfrak{W}}_2}{2}$ is invertible and strictly increasing. Based on this, let us introduce a mapping defined as follows:

$$\Phi(\tau) = \left(\sigma\mathcal{I} + \frac{\hat{\mathfrak{W}}_1 + \hat{\mathfrak{W}}_2}{2}\right)^{-1}(\hat{\sigma}\tau), \ \forall \tau \in \mathbb{R}, \quad (46)$$

for a constant $\hat{\sigma} > 0$, which is a strictly increasing, positive and continuous function with $\Phi(0) = 0$. Define

$$\Psi(\tau) = \tau - (\mathcal{I} + \Phi)^{-1}(\tau), \ \forall \tau \in \mathbb{R}. \quad (47)$$

Then $\Psi(\tau)$ is also a positive, continuous and strictly increasing function.

Lemma III.1. *([7]) If $\Phi(t) > 0$ for any $t > 0$ as defined in (46), then $\lim_{t\to\infty}\mathcal{S}(t) = 0$, where $S(\cdot)$ represents the solution of the corresponding ODE system:*

$$\begin{cases} \dfrac{\mathrm{d}}{\mathrm{d}t}\mathcal{S}(t) + \Psi(\mathcal{S}(t)) = 0, \quad t > 0, \\ \mathcal{S}(0) = \mathcal{S}_0. \end{cases} \quad (48)$$

Lemma III.2. *([30]) Let Φ be the mapping as defined in (46), and consider a sequence $\{\tau_n\}_n$ of positive numbers satisfying the given conditions.*

$$\Phi(\tau_{n+1}) + \tau_{n+1} \le \tau_n, \quad n \ge 0. \quad (49)$$

Then $\tau_n \le \mathcal{S}(n)$, where $\mathcal{S}$ is the solution of the ODE system (48).

To establish the stability result, we require several technical lemmas. To this end, let us define the following quantity:

$$C_\beta := \min\left\{\frac{3I + L\Lambda - 2\beta L\Lambda}{2I + 2\Lambda L}, 1\right\}, \quad (50)$$

where β is an adjustment parameter satisfying $0 < \beta < \frac{I}{L\Lambda}$. It is easy to check that $\frac{1}{2} < C_\beta \le 1$. Replace u in (16) with $x\Upsilon_x - \alpha\Upsilon$ ($\frac{1}{2} < \alpha < C_\beta$) to produce

$$\begin{aligned} &\underbrace{\rho\Lambda\int_0^L \Upsilon_{tt}(x\Upsilon_x - \alpha\Upsilon)dx}_{\mathcal{N}_1} + \underbrace{\rho I\int_0^L \Upsilon_{xtt}(x\Upsilon_x - \alpha\Upsilon)_x dx}_{\mathcal{N}_2} \\ &+\underbrace{\mathcal{E}I\int_0^L \Upsilon_{xx}(x\Upsilon_x - \alpha\Upsilon)_{xx}}_{\mathcal{N}_3} + \underbrace{F_1(\Upsilon_t(L,t))(x\Upsilon_x - \alpha\Upsilon)(L,t)}_{\mathcal{N}_5} \\ &+\underbrace{\int_0^L (\mathcal{E}\Lambda + \frac{P - \mathcal{E}\Lambda}{\sqrt{1 + \Upsilon_x^2}})\Upsilon_x(x\Upsilon_x - \alpha\Upsilon)_x dx}_{\mathcal{N}_4} \\ &+\underbrace{F_2(\Upsilon_{xt}(L,t))(x\Upsilon_x - \alpha\Upsilon)_x(L,t)}_{\mathcal{N}_6} = 0. \end{aligned} \quad (51)$$

Lemma III.3. *For $\mathcal{N}_1$, $\mathcal{N}_2$, and $\mathcal{N}_3$ defined in (51), the following holds:*

$$\begin{aligned}\mathcal{N}_1 &= \rho\Lambda\int_0^L [x\Upsilon_t\Upsilon_x - \alpha\Upsilon\Upsilon_t]_t dx - \frac{\rho\Lambda}{2}L\Upsilon_t^2(L,t)\\ &\quad +(\frac{1}{2}+\alpha)\rho\Lambda\int_0^L \Upsilon_t^2 dx, \end{aligned} \tag{52}$$

$$\mathcal{N}_3 = (\frac{3}{2}-\alpha)\mathcal{E}I\int_0^L \Upsilon_{xx}^2 dx + \frac{\mathcal{E}I}{2}L\Upsilon_{xx}^2(L,t), \tag{53}$$

$$\begin{aligned}\mathcal{N}_2 &= \rho I\int_0^L [(1-\alpha)\Upsilon_{xt}\Upsilon_x + x\Upsilon_{xt}\Upsilon_{xx}]_t dx\\ &\quad +(\alpha-\frac{1}{2})\rho I\int_0^L \Upsilon_{xt}^2 dx - \frac{\rho I}{2}L\Upsilon_{xt}^2(L,t). \end{aligned} \tag{54}$$

Proof: By performing integration by parts, we derive the following expression:

$$\begin{aligned}\int_0^L x\Upsilon_{tt}\Upsilon_x dx &= \int_0^L [x\Upsilon_t\Upsilon_x]_t dx - \int_0^L x\Upsilon_{xt}\Upsilon_t dx\\ &= \int_0^L [x\Upsilon_t\Upsilon_x]_t dx - \frac{1}{2}L\Upsilon_t^2(L,t) + \frac{1}{2}\int_0^L \Upsilon_t^2 dx, \end{aligned} \tag{55}$$

and

$$-\int_0^L \Upsilon_{tt}\Upsilon dx = -\int_0^L [\Upsilon\Upsilon_t]_t dx + \int_0^L \Upsilon_t^2 dx. \tag{56}$$

By adding equations (55) and (56), we obtain the desired result given in (52). Similar to the derivation of (55), we can deduce that

$$\begin{aligned}&\int_0^L \Upsilon_{xtt}(x\Upsilon_x - \alpha\Upsilon)_x dx\\ &= \int_0^L [(1-\alpha)\Upsilon_{xt}\Upsilon_x + x\Upsilon_{xt}\Upsilon_{xx}]_t - [x\Upsilon_{xt}\Upsilon_{xxt} + (1-\alpha)\Upsilon_{xt}^2] dx\\ &= \int_0^L [(1-\alpha)\Upsilon_{xt}\Upsilon_x + x\Upsilon_{xt}\Upsilon_{xx}]_t dx + (\alpha-\frac{1}{2})\int_0^L \Upsilon_{xt}^2 dx\\ &\quad -\frac{1}{2}L\Upsilon_{xt}^2(L,t), \end{aligned} \tag{57}$$

where the boundary condition (14d) was applied. According to (57), (54) is obtained. Similarly to (57), one can derive that

$$\mathcal{E}I\int_0^L \Upsilon_{xx}(x\Upsilon_x - \alpha\Upsilon)_{xx} = \mathcal{E}I\int_0^L \Upsilon_{xx}[x\Upsilon_{xxx} + (2-\alpha)\Upsilon_{xx}] dx, \tag{58}$$

and

$$\mathcal{E}I\int_0^L x\Upsilon_{xx}\Upsilon_{xxx} dx = -\frac{\mathcal{E}I}{2}\int_0^L \Upsilon_{xx}^2 dx + \frac{\mathcal{E}I}{2}L\Upsilon_{xx}^2(L,t). \tag{59}$$

By plugging (59) into (58), we can obtain (53). ■

Lemma III.4. *For $\mathcal{N}_4$, $\mathcal{N}_5$, and $\mathcal{N}_6$ defined in (51), the following holds:*

$$\begin{aligned}\mathcal{N}_4 &\geq (\frac{1}{2}-\alpha)\int_0^L \int_0^{\Upsilon_x^2} \big(\mathcal{E}\Lambda + \frac{P-\mathcal{E}\Lambda}{\sqrt{1+\theta}}\big) d\theta dx\\ &\quad +\frac{L}{2}\int_0^{\Upsilon_x^2(L,t)} \big(\mathcal{E}\Lambda + \frac{P-\mathcal{E}\Lambda}{\sqrt{1+\theta}}\big) d\theta, \end{aligned} \tag{60}$$

$$\begin{aligned}\mathcal{N}_5 &= \big[-\rho I\Upsilon_{xtt}(L,t) - \big(\mathcal{E}\Lambda + \frac{P-\mathcal{E}\Lambda}{\sqrt{1+\Upsilon^2(L,t)}}\big)\Upsilon_x(L,t)\\ &\quad +\mathcal{E}I\Upsilon_{xxx}(L,t)\big][L\Upsilon_x(L,t) - \alpha\Upsilon(L,t)], \end{aligned} \tag{61}$$

$$\mathcal{N}_6 = -\mathcal{E}IL\Upsilon_{xx}^2(L,t) - \mathcal{E}I(1-\alpha)\Upsilon_{xx}(L,t)\Upsilon_x(L,t). \tag{62}$$

Proof: Similarly to the derivation of (58), we can demonstrate that

$$\begin{aligned}&\int_0^L (\mathcal{E}\Lambda + \frac{P-\mathcal{E}\Lambda}{\sqrt{1+\Upsilon_x^2}})\Upsilon_x(x\Upsilon_x - \alpha\Upsilon)_x dx\\ &= (1-\alpha)\int_0^L (\mathcal{E}\Lambda + \frac{P-\mathcal{E}\Lambda}{\sqrt{1+\Upsilon_x^2}})\Upsilon_x^2 dx\\ &\quad +\frac{1}{2}\int_0^L \Big[x\int_0^{\Upsilon_x^2} \big(\mathcal{E}\Lambda + \frac{P-\mathcal{E}\Lambda}{\sqrt{1+\theta}}\big) d\theta\Big]_x dx\\ &\quad -\frac{1}{2}\int_0^L \int_0^{\Upsilon_x^2} \big(\mathcal{E}\Lambda + \frac{P-\mathcal{E}\Lambda}{\sqrt{1+\theta}}\big) d\theta dx. \end{aligned} \tag{63}$$

Let $y(\tau) := \mathcal{E}\Lambda + \frac{P-\mathcal{E}\Lambda}{\sqrt{1+\tau}}$, $\forall \tau \geq 0$. Since y is monotonically increasing for $\tau \geq 0$, $y(\tau) \geq y(0) > 0$ which leads to

$$\begin{aligned}\tau y(\tau) &= \tau(\mathcal{E}\Lambda + \frac{P-\mathcal{E}\Lambda}{\sqrt{1+\tau}}) \geq \int_0^\tau y(\theta) d\theta\\ &\geq \int_0^\tau \big(\mathcal{E}\Lambda + \frac{P-\mathcal{E}\Lambda}{\sqrt{1+\theta}}\big) d\theta \geq 0, \end{aligned} \tag{64}$$

for any $\tau \geq 0$. Substituting (64) into (63) yields (60). Additionally, using (14b) and (14c), we can effortlessly derive (61) and (62). ■

The stability is stated as Theorem III.1 following.

Theorem III.1. *Assuming that conditions (7a), (7b), and (44) are satisfied for the closed-loop system (14a)-(14e) with initial data $(\Upsilon_0, \Upsilon_1)^\top \in \mathcal{D}(\mathfrak{A})$, there exists a constant $T > 0$ such that*

$$\mathbb{E}(t) \leq \mathcal{S}\left(\frac{t}{T} - 1\right), \tag{65}$$

for all $t > T$ with $\lim_{t\to\infty} \mathcal{S}(t) = 0$, where $\mathcal{S}(\cdot)$ is the solution of ODE system (48) with $\mathcal{S}_0 = \mathbb{E}(0)$. Furthermore,

$$|\Upsilon(x,t)|^2 \leq \frac{2L}{\mathcal{E}I}\mathcal{S}\left(\frac{t}{T} - 1\right), \tag{66}$$

for all $t > T$ and $x \in [0, L]$.

Proof: By Lemmas III.3 and III.4, substituting (52)-(53)

and (60)-(62) into (51) yields

$$\begin{aligned}
&\beta\int_0^L\int_0^{\Upsilon_x^2}\big(\mathcal{E}\Lambda+\frac{P-\mathcal{E}\Lambda}{\sqrt{1+\theta}}\big)d\theta dx+(\alpha-\frac{1}{2})\rho I\int_0^L\Upsilon_{xt}^2dx\\
&+(\frac{1}{2}-\alpha-\beta)\int_0^L\int_0^{\Upsilon_x^2}\big(\mathcal{E}\Lambda+\frac{P-\mathcal{E}\Lambda}{\sqrt{1+\theta}}\big)d\theta dx\\
&\underbrace{+(\frac{1}{2}+\alpha)\rho\Lambda\int_0^L\Upsilon_t^2dx+(\frac{3}{2}-\alpha)\mathcal{E}I\int_0^L\Upsilon_{xx}^2dx}_{Q_1}\\
&\le\underbrace{-\int_0^L\big[\rho\Lambda(x\Upsilon_x-\alpha\Upsilon)\Upsilon_t+\rho I[(1-\alpha)\Upsilon_x+x\Upsilon_{xx}]\Upsilon_{xt}\big]_t dx}_{Q_2}\\
&+\underbrace{\Big[\Upsilon_x(L,t)(\mathcal{E}\Lambda+\frac{P-\mathcal{E}\Lambda}{\sqrt{1+\Upsilon_x^2(L,t)}})+\rho I\Upsilon_{xtt}(L,t)\\
&\quad-\mathcal{E}I\Upsilon_{xxx}(L,t)\Big][L\Upsilon_x(L,t)-\alpha\Upsilon(L,t)]}_{Q_3}\\
&+\underbrace{L\Big[\frac{\rho\Lambda}{2}\Upsilon_t^2(L,t)+\frac{\rho I}{2}\Upsilon_{xt}^2(L,t)+\frac{\mathcal{E}I}{2}\Upsilon_{xx}^2(L,t)\\
&\quad-\frac{1}{2}\int_0^{\Upsilon_x^2(L,t)}\big(\mathcal{E}\Lambda+\frac{P-\mathcal{E}\Lambda}{\sqrt{1+\theta}}\big)d\theta\Big]}_{Q_4}\\
&+\underbrace{(1-\alpha)\mathcal{E}I\Upsilon_x(L,t)\Upsilon_{xx}(L,t)}_{Q_5},
\end{aligned}\tag{67}$$

where the adjustment parameter β was introduced to specify the parameter range of the integral multiplier provided by (50). The corresponding term serves as an adjustment to construct the energy function.

Next, we will prove Theorem III.1 through five steps.

Step 1: For Q_1, the following holds:

$$\int_S^T Q_1dt\ge C_1\int_S^T\mathbb{E}(t)dt,\tag{68}$$

where $C_1=\min\big\{2\alpha-1,3-2\alpha+\frac{(1-2\alpha-2\beta)L\Lambda}{I},2\beta\big\}$ with the α and β being mentioned in (50).

Based on the inequality $P\le\mathcal{E}\Lambda$, we can derive $\mathcal{E}\Lambda+\frac{P-\mathcal{E}\Lambda}{\sqrt{1+\theta}}\le\mathcal{E}\Lambda,\ \forall\theta\ge0$. Furthermore, applying the e Poincaré inequality yields

$$\int_0^L\int_0^{\Upsilon_x^2}\big(\mathcal{E}\Lambda+\frac{P-\mathcal{E}\Lambda}{\sqrt{1+\theta}}\big)d\theta dx\le\mathcal{E}\Lambda L\int_0^L\Upsilon_{xx}^2dx.\tag{69}$$

Plug (69) into Q_1 to yield

$$\begin{aligned}
Q_1&\ge(\frac{1}{2}+\alpha)\rho\Lambda\int_0^L\Upsilon_t^2dx+(\alpha-\frac{1}{2})\rho I\int_0^L\Upsilon_{xt}^2dx\\
&\quad+[(\frac{3}{2}-\alpha)\mathcal{E}I+(\frac{1}{2}-\alpha-\beta)\mathcal{E}\Lambda L]\int_0^L\Upsilon_{xx}^2dx\\
&\quad+\beta\int_0^L\int_0^{\Upsilon_x^2}\big(\mathcal{E}\Lambda+\frac{P-\mathcal{E}\Lambda}{\sqrt{1+\theta}}\big)d\theta dx\\
&\ge C_1\mathbb{E}(t),
\end{aligned}\tag{70}$$

where C_1 is a constant defined in (68). It is straightforward to verify that C_1 is positive. By integrating both sides of (70) from S to T, we obtain (68).

Step 2: For Q_2, we obtain the following:

$$\int_S^T Q_2dt\le2C_2\mathbb{E}(S),\tag{71}$$

where $C_2=\max\big\{L^2+\alpha,\frac{[\rho\Lambda+(1-\alpha)\rho I]L+\alpha\rho\Lambda L^2+\rho I}{\mathcal{E}I}\big\}$.

By Cauchy's inequality, we can deduce that

$$\begin{aligned}
&\int_0^L[\rho\Lambda(x\Upsilon_x-\alpha\Upsilon)\Upsilon_t+\rho I[(1-\alpha)\Upsilon_x+x\Upsilon_{xx}]\Upsilon_{xt}]dx\\
&\le\frac{\rho\Lambda}{2}\int_0^L(L^2\Upsilon_t^2+\Upsilon_x^2)dx+\frac{\alpha\rho\Lambda}{2}\int_0^L(\Upsilon^2+\Upsilon_t^2)dx\\
&\quad+\frac{1-\alpha}{2}\rho I\int_0^L(\Upsilon_{xt}^2+\Upsilon_x^2)dx+\frac{\rho I}{2}\int_0^L(L^2\Upsilon_{xt}^2+\Upsilon_{xx}^2)dx\\
&\le\frac{L^2+\alpha}{2}\rho\Lambda\int_0^L\Upsilon_t^2dx+\frac{1-\alpha+L^2}{2}\rho I\int_0^L\Upsilon_{xt}^2dx\\
&\quad+\frac{[\rho\Lambda+(1-\alpha)\rho I]L+\alpha\rho\Lambda L^2+\rho I}{2}\int_0^L\Upsilon_{xx}^2dx\\
&\le C_2\mathbb{E}(t),
\end{aligned}\tag{72}$$

where C_2 is a constant defined in (71). For all $t\ge0$, the dissipation of the energy function $\mathbb{E}(t)$ stated in Lemma II.3 implies that

$$\begin{aligned}
\int_S^T Q_2dt&\le\Big|\int_0^L\rho\Lambda[x\Upsilon_x(x,T)-\alpha\Upsilon(x,T)]\Upsilon_t(x,T)\\
&\qquad+\rho I[(1-\alpha)\Upsilon_x(x,T)+x\Upsilon_{xx}(x,T)]\Upsilon_{xt}(x,T)dx\Big|\\
&\quad+\Big|\int_0^L\rho\Lambda[x\Upsilon_x(x,S)-\alpha\Upsilon(x,S)]\Upsilon_t(x,S)\\
&\qquad+\rho I[(1-\alpha)\Upsilon_x(x,S)+x\Upsilon_{xx}(x,S)]\Upsilon_{xt}(x,S)dx\Big|\\
&\le C_2(\mathbb{E}(T)+\mathbb{E}(S))\le2C_2\mathbb{E}(S).
\end{aligned}\tag{73}$$

Step 3: For Q_1, Q_2 and Q_3, we obtain

$$\begin{aligned}
&\int_S^T Q_3+Q_4+Q_5dt\\
&\le\int_S^T\Big[\frac{1}{4\eta}F_1^2(\Upsilon_t(x,t))+\frac{\rho\Lambda L}{2}\Upsilon_t^2(L,t)\Big]dt\\
&\quad+\int_S^T\Big[\frac{L+2\varepsilon}{2\mathcal{E}I}F_2^2(\Upsilon_{xt}(L,t))+\frac{\rho IL}{2}\Upsilon_{xt}^2(L,t)\Big]dt\\
&\quad+\Big[\frac{4\eta(L^3+\alpha^2L^2)}{\mathcal{E}I}+\frac{(1-\alpha)^2L}{2\varepsilon}\Big]\int_S^T\mathbb{E}(t)dt.
\end{aligned}\tag{74}$$

Next, applying Young's inequality ($\mathfrak{a}\mathfrak{b}\le\frac{\mathfrak{a}^2}{4\eta}+\eta\mathfrak{b}^2,\forall\eta>0$), the Cauchy-Schwarz inequality, and Poincaré inequality, we obtain:

$$\begin{aligned}
&\big|F_1(\Upsilon_t(L,t))L\Upsilon_x(L,t)-\alpha\Upsilon(L,t)]\big|\\
&\le\frac{1}{4\eta}F_1^2(\Upsilon_t(L,t))+\eta\big|L\Upsilon_x(L,t)-\alpha\Upsilon(L,t)\big|^2\\
&=\frac{1}{4\eta}F_1^2(\Upsilon_t(L,t))+\eta\Big|L\int_0^L\Upsilon_{xx}dx-\alpha\int_0^L\Upsilon_xdx\Big|^2\\
&\le\frac{1}{4\eta}F_1^2(\Upsilon_t(L,t))+2\eta(L^3+\alpha^2L^2)\int_0^L\Upsilon_{xx}^2dx,
\end{aligned}\tag{75}$$

where $\eta > 0$ is the Young's parameter. Using the boundary value condition (14d), we can determine that

$$\begin{aligned} Q_3 &= \Big[\Upsilon_x(L,t)(\mathcal{E}\Lambda + \frac{P-\mathcal{E}\Lambda}{\sqrt{1+\Upsilon_x^2(L,t)}}) - \mathcal{E}I\Upsilon_{xxx}(L,t) \\ &\quad +\rho I\Upsilon_{xtt}(L,t)\Big][L\Upsilon_x(L,t) - \alpha\Upsilon(L,t)] \\ &= -F_1(\Upsilon_t(L,t))[L\Upsilon_x(L,t) - \alpha\Upsilon(L,t)]. \end{aligned} \tag{76}$$

Substituting (75) into (76) results in the following estimation:

$$Q_3 \le \frac{1}{4\eta}F_1^2(\Upsilon_t(L,t)) + 2\eta(L^3+\alpha^2L^2)\int_0^L \Upsilon_{xx}^2 dx. \tag{77}$$

For Q_4, from (64),

$$\begin{aligned} Q_4 &= \frac{\rho\Lambda L}{2}\Upsilon_t^2(L,t) + \frac{\rho IL}{2}\Upsilon_{xt}^2(L,t) + \frac{\mathcal{E}IL}{2}\Upsilon_{xx}^2(L,t) \\ &\quad -L\int_0^{\Upsilon_x^2(L,t)}(\mathcal{E}\Lambda + \frac{P-\mathcal{E}\Lambda}{\sqrt{1+\theta}})d\theta \\ &\le \frac{\rho\Lambda L}{2}\Upsilon_t^2(L,t) + \frac{\rho IL}{2}\Upsilon_{xt}^2(L,t) + \frac{\mathcal{E}IL}{2}\Upsilon_{xx}^2(L,t). \end{aligned} \tag{78}$$

Likewise (75), we can derive that

$$\begin{aligned} Q_5 &= (1-\alpha)\mathcal{E}I\Upsilon_x(L,t)\Upsilon_{xx}(L,t) \\ &\le \frac{(1-\alpha)^2\mathcal{E}I}{4\varepsilon}\big|\Upsilon_x(L,t)\big|^2 + \varepsilon\mathcal{E}I\big|\Upsilon_{xx}(L,t)\big|^2 \\ &= \frac{(1-\alpha)^2\mathcal{E}I}{4\varepsilon}\left|\int_0^L \Upsilon_{xx}dx\right|^2 + \varepsilon\mathcal{E}I\Upsilon_{xx}^2(L,t) \\ &\le \frac{(1-\alpha)^2\mathcal{E}IL}{4\varepsilon}\int_0^L \Upsilon_{xx}^2 dx + \varepsilon\mathcal{E}I\Upsilon_{xx}^2(L,t), \end{aligned} \tag{79}$$

where $\varepsilon > 0$ is the Young's parameter. By adding up (77), (78), and (79), and applying the boundary conditions (14d) and (14b), we integrate both sides from S to T to arrive at (74).

Step 4: There is the following:

$$\begin{aligned} \mathbb{E}(T) \le \mathfrak{C}_1\int_0^T [\Upsilon_t^2(L,t) + F_1^2(\Upsilon_t(L,t))]dt \\ +\mathfrak{C}_2\int_0^T [\Upsilon_{xt}^2(L,t) + F_2^2(\Upsilon_{xt}(L,t))]dt, \end{aligned} \tag{80}$$

where $\mathfrak{C}_1 = \frac{2C_2+2\hat{C}_1}{C_1T-4C_2}$ and $\mathfrak{C}_2 = \frac{2C_2+2\hat{C}_2}{C_1T-4C_2}$.

Integrating both sides of (67) from S to T and substituting (68), (73), and (74) into the result yields:

$$\begin{aligned} &C_1\int_S^T \mathbb{E}(t)dt \\ &\le 2C_2\mathbb{E}(S) + \Big[\frac{4\eta(L^3+\alpha^2L^2)}{\mathcal{E}I} + \frac{(1-\alpha)^2L}{2\varepsilon}\Big]\int_S^T \mathbb{E}(t)dt \\ &\quad +\hat{C}_1\int_S^T F_1^2(\Upsilon_t(L,t)) + \Upsilon_t^2(L,t)dt \\ &\quad +\hat{C}_2\int_S^T F_2^2(\Upsilon_{xt}(L,t)) + \Upsilon_{xt}^2(L,t)dt, \end{aligned} \tag{81}$$

where C_1 and C_2 are the constants given by (70) and (72), respectively, $\hat{C}_1 = \max\{\frac{1}{4\eta}, \frac{\rho\Lambda L}{2}\}$ and $\hat{C}_2 = \max\{\frac{L+2\varepsilon}{2\mathcal{E}I}, \frac{\rho IL}{2}\}$. Since the Young's parameter η and ε are arbitrary, we can choose $\eta = \frac{C_1\mathcal{E}I}{16(L^3+\alpha^2L^2)}$ and $\varepsilon = \frac{2(1-\alpha)^2L}{C_1}$. Substituting the selected parameters into equation (81) gives

$$\begin{aligned} \int_S^T \mathbb{E}(t)dt &\le \frac{2\hat{C}_1}{C_1}\int_S^T [F_1^2(\Upsilon_t(L,t)) + \Upsilon_t^2(L,t)]dt \\ &\quad +\frac{2\hat{C}_2}{C_1}\int_S^T [F_2^2(\Upsilon_{xt}(L,t)) + \Upsilon_{xt}^2(L,t)]dt + \frac{4C_2}{C_1}\mathbb{E}(S). \end{aligned} \tag{82}$$

Letting $S = 0$ and $T > 0$ in (82), we immediately obtain that

$$\begin{aligned} \int_S^T \mathbb{E}(t)dt &\le \frac{2\hat{C}_1}{C_1}\int_0^T [F_1^2(\Upsilon_t(L,t)) + \Upsilon_t^2(L,t)]dt \\ &\quad +\frac{2\hat{C}_2}{C_1}\int_0^T [F_2^2(\Upsilon_{xt}(L,t)) + \Upsilon_{xt}^2(L,t)]dt + \frac{4C_2}{C_1}\mathbb{E}(0). \end{aligned} \tag{83}$$

Thanks to

$$\begin{aligned} \mathbb{E}(T) = \mathbb{E}(S) - \int_S^T F_1(\Upsilon_t(L,t))\Upsilon_t(L,t)dt \\ -\int_S^T F_2(\Upsilon_{xt}(L,t))\Upsilon_{xt}(L,t)dt, \end{aligned} \tag{84}$$

which is derived by integrating both sides of (34) from S to T. Consequently, one arrives at:

$$\begin{aligned} \mathbb{E}(0) \le \mathbb{E}(T) + \frac{1}{2}\int_0^T [F_1^2(\Upsilon_t(L,t)) + \Upsilon_t^2(L,t)]dt \\ +\frac{1}{2}\int_0^T [F_2^2(\Upsilon_{xt}(L,t)) + \Upsilon_{xt}^2(L,t)]dt. \end{aligned} \tag{85}$$

Substituting (85) into (83) gives

$$\begin{aligned} \int_0^T \mathbb{E}(t)dt \le \frac{4C_2}{C_1}\mathbb{E}(T) \\ +\frac{2(C_2+\hat{C}_1)}{C_1}\int_0^T [F_1^2(\Upsilon_t(L,t)) + \Upsilon_t^2(L,t)]dt \\ +\frac{2(C_2+\hat{C}_2)}{C_1}\int_0^T [F_2^2(\Upsilon_{xt}(L,t)) + \Upsilon_{xt}^2(L,t)]dt. \end{aligned} \tag{86}$$

The monotonic non-increasing nature of the energy function $\mathbb{E}(t)$ indicates that $\int_0^T \mathbb{E}(t)dt \ge T\mathbb{E}(T)$. Therefore, for $T > \frac{4C_2}{C_1}$, and by referring to equation (86), we have successfully derived equation (80).

Step 5: There holds

$$\Phi(\mathbb{E}(T)) + \mathbb{E}(T) \le \mathbb{E}(0), \tag{87}$$

where Φ is defined by (46).

Denote $\varphi := \{t \in [0,T]; |\Upsilon_t(L,t)| \le \mu\}$ and $\phi := \{t \in [0,T]; |\Upsilon_{xt}(L,t)| \le \mu\}$ with the constant μ provided in (7b). By (7b), it is straightforward to obtain

$$\begin{aligned} \int_{[0,T]\setminus\varphi} [\Upsilon_t^2(L,t) + F_1^2(\Upsilon_t(L,t))]dt \\ \le \hat{C}_3\int_{[0,T]\setminus\varphi} \Upsilon_t(L,t)F_1(\Upsilon_t(L,t))dt, \end{aligned} \tag{88}$$

with $\hat{C}_3 = \frac{1+b^2}{a}$. Analogously, it can be observed that

$$\begin{aligned} \int_{[0,T]\setminus\phi} [\Upsilon_{xt}^2(L,t) + F_2^2(\Upsilon_{xt}(L,t))]dt \\ \le \hat{C}_3\int_{[0,T]\setminus\phi} \Upsilon_{xt}(L,t)F_2(\Upsilon_{xt}(L,t))dt. \end{aligned} \tag{89}$$

On the other hand, the equation (44) yields

$$\int_{\varphi}[\Upsilon_t^2(L,t)+F_1^2(\Upsilon_t(L,t))]dt \le \int_{\varphi}\mathfrak{W}_1(\Upsilon_t(L,t)F_1(\Upsilon_t(L,t)))dt, \tag{90}$$

and

$$\int_{\phi}[\Upsilon_{xt}^2(L,t)+F_2^2(\Upsilon_{xt}(L,t))]dt \le \int_{\phi}\mathfrak{W}_2(\Upsilon_{xt}(L,t)F_2(\Upsilon_{xt}(L,t)))dt. \tag{91}$$

Applying Jensen's inequality, we derive

$$\int_{\varphi}\mathfrak{W}_1(\Upsilon_t(L,t)F_1(\Upsilon_t(L,t)))dt \le T\mathfrak{W}_1\Big(\int_0^T\frac{\Upsilon_t(L,t)F_1(\Upsilon_t(L,t))}{T}dt\Big)\le T\hat{\mathfrak{W}}_1(\Delta), \tag{92}$$

and

$$\int_{\phi}\mathfrak{W}_2(\Upsilon_{xt}(L,t)F_2(\Upsilon_{xt}(L,t)))dt \le T\mathfrak{W}_2\Big(\int_0^T\frac{\Upsilon_{xt}(L,t)F_2(\Upsilon_{xt}(L,t))}{T}dt\Big)\le T\hat{\mathfrak{W}}_2(\Theta), \tag{93}$$

where $\Delta := \int_0^T\Upsilon_t(L,t)F_1(\Upsilon_t(L,t))dt$ and $\Theta := \int_0^T\Upsilon_{xt}(L,t)F_2(\Upsilon_{xt}(L,t))dt$. By substituting (88), (89), (92), and (93) into (80), we obtain

$$\mathbb{E}(T)\le \mathfrak{C}_1T\hat{\mathfrak{W}}_1(\Delta)+\mathfrak{C}_2T\hat{\mathfrak{W}}_2(\Theta)+\mathfrak{C}_1\hat{C}_3\Delta+\mathfrak{C}_2\hat{C}_3\Theta. \tag{94}$$

Given that the functions $\hat{\mathfrak{W}}_i(\tau), i=1,2$ are concave and strictly increasing for $\tau\ge 0$, it can be inferred from (94) that

$$\begin{aligned}\mathbb{E}(T)&\le 2\mathfrak{C}_1T\hat{\mathfrak{W}}_1\big(\frac{1}{2}\Delta+\frac{1}{2}\Theta\big)+2\mathfrak{C}_2T\hat{\mathfrak{W}}_2\big(\frac{1}{2}\Delta+\frac{1}{2}\Theta\big)\\&\quad+\mathfrak{C}_1\hat{C}_3\Delta+\mathfrak{C}_2\hat{C}_3\Theta\\&\le \mathcal{K}_1\Big(\frac{\hat{\mathfrak{W}}_1+\hat{\mathfrak{W}}_2}{2}\Big)\Big(\frac{1}{2}\Delta+\frac{1}{2}\Theta\Big)+\mathcal{K}_2\Big(\frac{1}{2}\Delta+\frac{1}{2}\Theta\Big),\end{aligned} \tag{95}$$

where $\mathcal{K}_1=4\max\{\mathfrak{C}_1T,\mathfrak{C}_2T\}$, $\mathcal{K}_2=2\max\{\mathfrak{C}_1\hat{C}_3,\mathfrak{C}_2\hat{C}_3\}$ and the map $\frac{\hat{\mathfrak{W}}_1+\hat{\mathfrak{W}}_2}{2}$ is defined in (46). By setting

$$\hat{\sigma}=\frac{2}{\mathcal{K}_1},\sigma=\frac{2\mathcal{K}_2}{\mathcal{K}_1}, \tag{96}$$

in (46), the estimate (95) is transformed into (87).

Since the estimate above remains valid in successive intervals $[nT,(n+1)T]$, we can deduce from (87) that

$$\Phi(\mathbb{E}(n+1)T)+\mathbb{E}((n+1)T)\le\mathbb{E}(nT),\quad n=0,1,2,\cdots. \tag{97}$$

Applying Lemma III.2 to the sequence $\tau_n=\mathbb{E}(nT)$ yields

$$\mathbb{E}(nT)\le S(n),\quad n=0,1,2,\cdots. \tag{98}$$

For any $t>0$, we can express t as $t=nT+\theta$, where n is an integer and $0\le\theta<T$. Consequently,

$$\mathbb{E}(t)\le\mathbb{E}(nT)\le S(n)\le S\left(\frac{t-\theta}{T}\right)\le S\left(\frac{t}{T}-1\right). \tag{99}$$

Using the boundary condition (14d), the Cauchy-Schwarz inequality, and the Poincaré inequality, we derive:

$$\begin{aligned}|\Upsilon(x,t)|^2&=\Big(\int_0^x\Upsilon_x(\tau,t)d\tau\Big)^2\le\Big(\int_0^L|\Upsilon_x(x,t)|dx\Big)^2\\&\le\int_0^L|\Upsilon_x(x,t)|^2dx\le L\int_0^L|\Upsilon_{xx}(x,t)|^2dx\le\frac{2L}{\mathcal{E}I}\mathbb{E}(t),\end{aligned}$$

for all $t>T$ and $x\in[0,L]$. The result can then be obtained by substituting (99) into the last inequality. ■

B. *Decay rate of closed-loop system*

In this section, we provide an estimated formula for the decay behavior by approximating (48), implying employ an idea from [30]. To obtain the solution of (48), which represents the estimated formula for decay behaviors, the crucial step is to construct concave functions $\mathfrak{W}_i(\cdot)$ as defined by (44). References [7] and [31] introduced a method for constructing the function $\mathfrak{W}^{-1}(\cdot)$ in the context of wave equations. The construction of these functions depends on the specific growth patterns of the strictly monotonic increasing functions $F_i(\cdot)$ near zero. Due to (44), our analysis can be restricted to positive values of τ.

We construct $\mathfrak{W}_i^{-1}(\tau)$ for $i=1,2$ as follows: If $F_i(\tau)$ decays to zero faster than a linear function on $0<\tau<\mu$ such as $\tau^3e^{-\frac{1}{\tau^2}}$, we let $\mathfrak{W}_i^{-1}(\tau):=\tau^{\frac{1}{2}}F_i(\tau^{\frac{1}{2}})$ for $i=1,2$. This ensures that $\mathfrak{W}_i(\tau F_i(\tau))=\tau^2$ satisfies (44). If $F_i(\tau)$ decays slower than a linear function on $0<\tau<\mu$, like $\tau^{\frac{1}{p}}$ with $p>1$, we let $\mathfrak{W}_i^{-1}(\tau):=\tau^{\frac{1}{2}}F_i^{-1}(\tau^{\frac{1}{2}})$ for $i=1,2$. In this case, $\mathfrak{W}_i(\tau F_i(\tau))=[F_i(\tau)]^2$ meets the condition (44). By adhering to these constructions, we can acquire the desired estimated formula that characterizes the decay behavior of both the solution and the energy.

In what follows, we will outline a method for estimating the decay rate, which is based on monotonic non-decreasing continuous functions that exhibit specific behaviors near zero such as

$$F_i(\tau)=\begin{cases}\mathbb{G}_i(\tau), & 0<\tau\le\varepsilon_0,\\ \mathbb{G}_i(\varepsilon_0), & \varepsilon_0<\tau<\mu,\end{cases} \tag{100}$$

where $\mathbb{G}_i(\tau)$ are strictly monotonically increasing on $0<\tau\le\mu=1$. The two types of growth forms of $F_i(\cdot)$ near zero are depicted in Figure 2. Using (100) as an example, let us introduce the construction method of $\mathfrak{W}_i^{-1}(\tau)$. When $F_i(\tau)$ decays faster than a linear function over $0<\tau\le\varepsilon_0$, similar to case I shown in Figure 2, we let $\mathfrak{W}_i^{-1}(\tau):=\tau^2F_i(\tau^{\frac{1}{2}})$ for $i=1,2$ to satisfy convexity. It can be deduced from $\tau^2=\mathfrak{W}_i(\tau^4F_i(\tau))\le\mathfrak{W}_i(\tau F_i(\tau))$ that $\tau^2\le\mathfrak{W}_i(\tau F_i(\tau))$ for $0<\tau<\mu$. In this case, this construction method leads to (44). When $F_i(\tau)$ decays slower than a linear function over $0<\tau<\mu$, similar to case II shown in Figure 2, we define $\mathfrak{W}_i^{-1}(\tau):=\tau^{\frac{1}{2}}\mathbb{G}_i^{-1}(\tau^2)$ for $i=1,2$ to ensure convexity. It is evident that $\mathbb{G}_i^2(\tau)\le\mathfrak{W}_i(\tau\mathbb{G}_i(\tau))$ can be derived from $\tau^2=\mathfrak{W}_i(\tau\mathbb{G}_i^{-1}(\tau^4))\le\mathfrak{W}_i(\tau\mathbb{G}_i^{-1}(\tau))$ for $0<\tau\le\varepsilon_0$. Furthermore, it follows that $\mathbb{G}_i^2(\varepsilon_0)\le\mathfrak{W}_i(\varepsilon_0\mathbb{G}_i(\varepsilon_0))\le\mathfrak{W}_i(\tau\mathbb{G}_i(\varepsilon_0))$ for $\varepsilon_0<\tau<\mu$ Consequently, $F_i^2(\tau)\le\mathfrak{W}_i(\tau F_i(\tau))$ holds on $0<\tau<\mu$, satisfying (44).

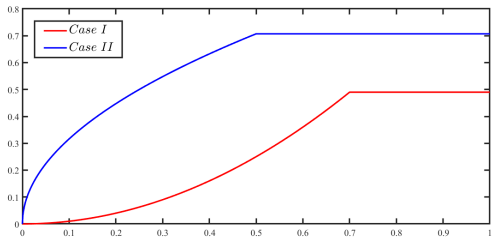

Fig. 2. Schematic representations of non-decreasing continuous functions near zero point.

Based on the argument presented in [7], obtaining the outcome of the algorithm is straightforward:

$$\Psi(\tau)=\hat{\sigma}^{-1}\Big(\mathcal{C}_0\mathcal{I}+\frac{\hat{\mathfrak{W}}_1+\hat{\mathfrak{W}}_2}{2}\Big)^{-1}(\tau), \tag{101}$$

with some constant $\mathcal{C}_0>0$. Therefore, it can be deduced from (101) that

$$\Psi(\tau)\sim\left(\mathcal{C}_0 I+\frac{\mathfrak{W}_1+\mathfrak{W}_2}{2}\right)^{-1}(\tau)\geq\mathcal{C}_1\left(\frac{\mathfrak{W}_1+\mathfrak{W}_2}{2}\right)^{-1}(\tau), \tag{102}$$

near the origin for some positive constant $\mathcal{C}_1$. It is straightforward to observe that

$$\mathcal{C}_1\left(\frac{\mathfrak{W}_1+\mathfrak{W}_2}{2}\right)^{-1}(\tau)\sim\mathcal{C}\left(\frac{\mathfrak{W}_1^{-1}+\mathfrak{W}_2^{-1}}{2}\right)(\tau)$$

close to the origin, for some positive constant C that is closely related to the initial value, as approximately depicted in Figure 3. It can be deduced from (102) that

$$\Psi(\tau)\geq\mathcal{C}\left(\frac{\mathfrak{W}_1^{-1}+\mathfrak{W}_2^{-1}}{2}\right)(\tau),$$

near the origin. Therefore, the asymptotic behavior of the solution and energy is governed by the following ODE:

$$\begin{cases}\dfrac{\mathrm{d}}{\mathrm{d}t}\mathcal{S}(t)+\mathcal{C}\Big[\dfrac{\mathfrak{W}_1^{-1}(\mathcal{S}(t))+\mathfrak{W}_2^{-1}(\mathcal{S}(t))}{2}\Big]=0,\ t>0,\\ \mathcal{S}(0)=\mathcal{S}_0,\end{cases} \tag{103}$$

as claimed above. Thus, it follows from Theorem III.1 that $|\Upsilon(x,t)|^2\leq\frac{2L}{\mathcal{E}I}\mathbb{E}(t)\leq\frac{2LC_{\mathbb{E}(0)}}{\mathcal{E}I}\mathcal{S}(t)$, for all $t>0$ and $x\in[0,L]$, where $\mathcal{S}(t)$ is the solution of the ODE (103) and $\mathcal{S}_0=\mathbb{E}(0)$. It is worth noting that $\left(\frac{\mathfrak{W}_1^{-1}+\mathfrak{W}_2^{-1}}{2}\right)(\cdot)$ offers a significantly better approximation to the function $\Psi(\cdot)$ compared to $(\mathfrak{W}_1+\mathfrak{W}_2)^{-1}(\cdot)$. This superior approximation allows for the derivation of a more accurate decay rate estimation formula, as given in (103). Now we give some examples for different types of decay forms by solving the ODE (103) when different types of growth forms of nonlinear feedback functions near zero are available.

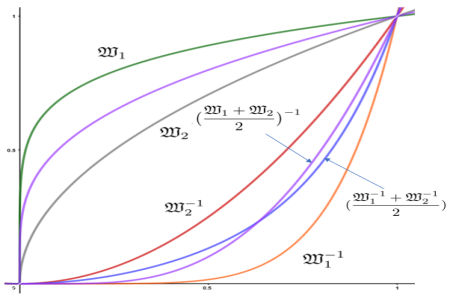

Fig. 3. Schematic representation of the construction of convex functions.

C. F_1 and F_2 exhibit the same type of change behavior near zero.

For this case, we present three illustrative examples.

Example III.1. *Consider $F_1(\tau)=m_1\tau^p$ (or $F_1(\tau)=m_1\tau^{\frac{1}{p}}$) and $F_2(\tau)=n_1\tau^p$ (or $F_2(\tau)=n_1\tau^{\frac{1}{p}}$) near zero, where $m_1,n_1>0$, $p>1$ are the constants. Set*

$$\mathfrak{W}_1^{-1}(\tau)=m_1\tau^{\frac{p+1}{2}},\quad \mathfrak{W}_2^{-1}(\tau)=n_1\tau^{\frac{p+1}{2}},$$

which are convex for $\tau>0$. From (103), solve the following ODE

$$\begin{cases}\dfrac{\mathrm{d}}{\mathrm{d}t}\mathcal{S}(t)+\dfrac{m_1}{2}\mathcal{S}(t)^{\frac{p+1}{2}}+\dfrac{n_1}{2}\mathcal{S}(t)^{\frac{p+1}{2}}=0,\quad t>0,\\ \mathcal{S}(0)=\mathcal{S}_0,\end{cases} \tag{104}$$

to obtain

$$\mathcal{S}(t)=\left[\mathcal{S}_0^{\frac{1-p}{2}}-\frac{(1-p)(m_1+n_1)}{4}t\right]^{\frac{2}{1-p}}.$$

Using $\mathcal{S}_0=\mathbb{E}(0)$ and Theorem III.1, we can derive the following conclusion:

$$\mathbb{E}(t)\leq C_{\mathbb{E}(0)}\left[\mathbb{E}(0)^{\frac{1-p}{2}}+\frac{(p-1)(m_1+n_1)}{4}t\right]^{\frac{2}{1-p}},$$

for all $t>0$ and $x\in[0,L]$. In particular, when $p=1$, by (104) we have

$$|\Upsilon(x,t)|^2\leq\frac{2L\mathbb{E}(t)}{\mathcal{E}I}\leq\frac{2LC_{\mathbb{E}(0)}}{\mathcal{E}I}e^{-\frac{m_1+n_1}{2}t},$$

This is consistent with the findings in [24] when considering two linear feedbacks, for all $t>0$ and $x\in[0,L]$.

Example III.2. *In this example, $F_1(\tau)=m_2\tau^{2p+1}e^{-\frac{1}{\tau^{2p}}}$ and $F_2(\tau)=n_2\tau^{2p+1}e^{-\frac{1}{\tau^{2p}}}$ near zero with positive constants m_1, n_2 and p. Let*

$$\mathfrak{W}_1^{-1}(\tau)=m_2\tau^{p+1}e^{-\frac{1}{\tau^p}},\ \mathfrak{W}_2^{-1}(\tau)=n_2\tau^{p+1}e^{-\frac{1}{\tau^p}}, \tag{105}$$

be convex functions for $\tau>0$. Substitute (105) into (103) and solve this ODE

$$\begin{cases}\dfrac{\mathrm{d}}{\mathrm{d}t}\mathcal{S}(t)+\dfrac{m_2+n_2}{2}\mathcal{S}(t)^{p+1}e^{-\frac{1}{\mathcal{S}(t)^p}}=0,\quad t>0,\\ \mathcal{S}(0)=\mathbb{E}(0),\end{cases}$$

to give

$$\mathbb{E}(t)\leq C_{\mathbb{E}(0)}\Big[\ln[e^{\frac{1}{\mathbb{E}(0)^p}}+\frac{(m_2+n_2)p}{2}t]\Big]^{-\frac{1}{p}},$$

for all $t>0$. This demonstrates that the solution and energy decay in a polynomial-logarithmic fashion.

Example III.3. *In this example, $F_i(\tau) = k_i\mathbb{F}(\tau)$, $i = 1, 2$, where $\mathbb{F}(\tau)$ is an odd function near zero and $k_i > 0$ are the constants, defined by*

$$\mathbb{F}(\tau) = \begin{cases} \tau^p, & 0 \le \tau \le \varepsilon_0, \\ \varepsilon_0^p, & \varepsilon_0 < \tau < 1, \end{cases} \tag{106}$$

with $p > 1$ being constant. Set

$$\mathfrak{W}_i^{-1}(\tau) = \begin{cases} k_i\tau^{\frac{p+4}{2}}, & 0 < \tau \le \varepsilon_0^2, \\ k_i\varepsilon_0^p\tau^2, & \varepsilon_0^2 < \tau < 1, \end{cases} \tag{107}$$

which are convex functions. By substituting (107) into (103) and solving the ordinary differential equation (ODE) piecewise, we obtain:

$$\mathcal{S}(t) = \begin{cases} \left[\mathbb{E}(0)^{-\frac{p+2}{2}} + \dfrac{(p+2)(k_1+k_2)}{4}t\right]^{-\frac{2}{p+2}}, & 0 < t \le C_{\varepsilon_0}, \\ \left[\widetilde{C}_{\varepsilon_0} + \dfrac{k_1+k_2}{2}\varepsilon_0^p t\right]^{-1}, & t > C_{\varepsilon_0}, \end{cases}$$

where C_{ε_0} is a constant related to ε_0 and $\widetilde{C}_{\varepsilon_0} = \left[\mathbb{E}(0)^{-\frac{p+2}{2}} + \frac{(p+2)(k_1+k_2)}{4}C_{\varepsilon_0}\right]^{\frac{2}{p+2}} - \frac{k_1+k_2}{2}\varepsilon_0^p C_{\varepsilon_0}$. This implies that

$$\mathbb{E}(t) \le C_{\mathbb{E}(0)}\left[\mathbb{E}(0)^{-\frac{p+2}{2}} + \frac{(p+2)(k_1+k_2)}{4}t\right]^{-\frac{2}{p+2}},$$

for all $t > 0$.

D. F_1 and F_2 exhibit different types of change behavior near zero.

In this case, we provide two illustrative examples.

Example III.4. *Let $F_1(\tau) = m_4\tau^p$ and $F_2(\tau) = n_4\tau$ near zero with constants $m_4, n_4 > 0$ and $p > 1$. Take*

$$\mathfrak{W}_1^{-1}(\tau) = m_4\tau^{\frac{p+1}{2}}, \ \mathfrak{W}_2^{-1}(\tau) = n_4\tau,$$

to be convex for $\tau > 0$. Solving the ODE

$$\begin{cases} \dfrac{\mathrm{d}}{\mathrm{d}t}\mathcal{S}(t) + \dfrac{m_4}{2}\mathcal{S}(t)^{\frac{p+1}{2}} + \dfrac{n_4}{2}\mathcal{S}(t) = 0, \quad t > 0, \\ \mathcal{S}(0) = \mathbb{E}(0), \end{cases}$$

gives

$$\mathbb{E}(t) \le C_{\mathbb{E}(0)}\left[\left[\mathbb{E}(0)^{\frac{1-p}{2}} + \frac{m_4}{n_4}\right]e^{-\frac{(1-p)n_4}{4}t} - \frac{m_4}{n_4}\right]^{\frac{2}{1-p}},$$

for all $t > 0$.

Example III.5. *Suppose that $F_1(\tau) = m_5\tau^{2p+1}e^{-\frac{1}{\tau^{2p}}}$ and $F_2(\tau) = n_5\tau^{2p+1}$ near zero, where m_5, n_5, p are positive constants. The convex functions can be taken as*

$$\mathfrak{W}_1^{-1}(\tau) = m_5\tau^{p+1}e^{-\frac{1}{\tau^p}}, \ \mathfrak{W}_2^{-1}(\tau) = n_5\tau^{p+1}, \ \forall\tau > 0.$$

By solving

$$\begin{cases} \dfrac{\mathrm{d}}{\mathrm{d}t}\mathcal{S}(t) + \dfrac{m_5}{2}\mathcal{S}(t)^{p+1}e^{-\frac{1}{\mathcal{S}(t)^p}} + \dfrac{n_5}{2}\mathcal{S}(t)^{p+1} = 0, \quad t > 0, \\ \mathcal{S}(0) = \mathbb{E}(0), \end{cases}$$

one obtains, for all $t > 0$, that

$$\mathbb{E}(t) \le C_{\mathbb{E}(0)}\left[\ln[(e^{\frac{1}{\mathbb{E}(0)^p}} + \frac{m_5}{n_5})e^{\frac{n_5 p}{2}t} - \frac{m_5}{n_5}]\right]^{-\frac{1}{p}}.$$

From the above examples, it is evident that the exponential decay is the most rapid, while the logarithmic-polynomial decay corresponding to Example III.2 is the slowest. The other forms of decay fall within this range.

IV. Numerical Simulations

In this section, we present simulation examples for the closed-loop system (14a)-(14e) to demonstrate the effectiveness of the proposed control (6). The simulations are conducted using the finite element method, with the quadratic Lagrangian basis of the finite element isometric grid employed. While the specific discrete equation of the closed-loop system is similar to the one presented in [10], it is omitted here for brevity. To illustrate the numerical results, the parameters of the closed-loop system (14a)-(14e) are listed in the following table.

Parameter	Definition	Value	Unit
L	Length	100	m
d_0	Outer diameter	0.4	m
ρ	Mass density	8200	kg/m^3
$\mathcal{E}$	Young's modulus	2×10^8	kg/m^2
P	Initial tension	6×10^4	N
I	Second moment	1.256×10^{-3}	m^4
Λ	Cross section area	1.256×10^{-3}	m^2

The initial displacement and velocity of the flexible riser used in the simulation are randomly set as $\Upsilon_0(x) = 1.5\sin 4x$ and $\Upsilon_1(x) = 3\cos 3x$ to represent the waveform of an elastic vibration system. For the simulations, various nonlinear feedback functions that meet the criteria (7a) and (7b) with =1 are implemented. These feedback functions are illustrated in Fig. 4.

$$G_1(\tau) = \begin{cases} \tau - 1, & \tau \le -1, \\ 2\tau, & -1 < \tau < 1, \\ \sin(\tau - 1) + 3\tau - 1, & \tau \ge 1, \end{cases} \tag{108}$$

$$G_2(\tau) = \begin{cases} 3\tau + \sin(\tau + 1) + 1, & \tau \le -1, \\ 2\tau^3, & -1 < \tau < 1, \\ \tau^2 + \tau, & 1 \le \tau < 3, \\ 3\tau + 3, & \tau \ge 3, \end{cases} \tag{109}$$

$$G_3(\tau) = \begin{cases} 2\tau - \dfrac{1}{e} + 2, & \tau \le -1, \\ \tau^3 e^{-\frac{1}{\tau^2}}, & -1 < \tau \le 1, \\ 5\tau + \dfrac{1}{e} + \ln[(\tau - 1)^2 + 1] - 5, & \tau > 1, \end{cases} \tag{110}$$

$$G_4(\tau) = \begin{cases} 2\tau - \dfrac{2}{e} + 2, & \tau \le -1, \\ 2\tau^5 e^{-\frac{1}{\tau^4}}, & -1 < \tau < 1, \\ \dfrac{2}{e} + 6\tau + \cos(\tau - 1) - 7, & \tau \ge 1. \end{cases} \tag{111}$$

The transverse displacements $\Upsilon(\cdot,\cdot)$ and the norm $\|\Upsilon(\cdot,t)\|$ of the closed-loop system (14a)-(14e), along with the corresponding control inputs $F_1(\cdot)$ and $F_2(\cdot)$ for three control schemes, are presented in Figs. 5-7. As observed from these figures, the decay behaviors of the nonlinear flexible marine riser system align with the theoretical results derived in Section

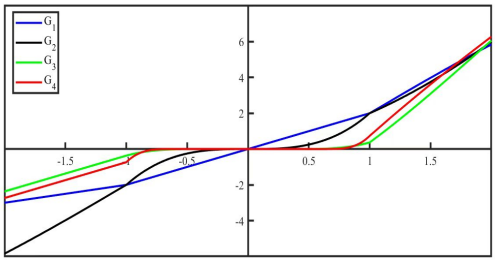

Fig. 4. The boundary feedback laws in simulation.

III. Specifically, the exponential decay (depicted in Fig. 5) exhibits the fastest rate, whereas the logarithmic-polynomial decay (shown in Fig. 7) is the slowest. The other forms of decay (illustrated in Fig. 6) fall within this range. In Fig. 6, a disturbance of the random square wave signal was implemented in our MATLAB simulation through the integration of a Random Number Module, which shows that the control scheme possesses a certain level of robustness. For a more detailed discussion on the practical implementation of this control system, we refer to [15].

V. Conclusions

This paper focuses on the stabilization of a nonlinear flexible marine riser system utilizing double nonlinear boundary controls. Starting from the Hamilton's principle, a nonlinear PDE model for the flexible marine riser system, incorporating rotational inertia, is derived. The nonlinear semigroup approach is employed to establish the well-posedness of the resulting closed-loop system, ensuring that the solution depends continuously on the initial data.

To determine an appropriate integral multiplier, an adjustment term is introduced, allowing for the identification of the existence range of the integral multiplier parameter. Under a broader set of feedback controls, the asymptotic stability of the closed-loop system is achieved by solving a dissipative ODE. Furthermore, the decay behaviors of both the solutions and the energy function for the closed-loop system are estimated.

Future work will aim to extend this method to tackle even more nonlinear controls in PDEs, particularly those encountered in the nonlinear flexible marine riser system with thermal effects. Such extensions will enhance our understanding and capabilities in controlling complex nonlinear systems, with potential applications in various engineering fields. In addition, the same stability properties cannot be achieved when dealing with weak solutions due to their lack of regularity. This issue is purely mathematical and requires further investigation.

Appendix

In this section, we will derive the system model. By referring to equations (8) and (9), we can deduce the variational form of the kinetic energy $\mathcal{K}$ and the potential energy $\mathcal{U}$ as follows:

$$\delta\mathcal{K}(t) = \rho I \int_0^L \Upsilon_{xt}(\delta\Upsilon)_{xt}dx + \rho\Lambda \int_0^L \Upsilon_t(\delta\Upsilon)_t dx, \quad (112)$$

and

$$\delta\mathcal{U}(t) = (P-\mathcal{E}\Lambda)\int_0^L \frac{\Upsilon_x(\delta\Upsilon)_x}{\sqrt{1+\Upsilon_x^2}}dx + \mathcal{E}\Lambda\int_0^L \Upsilon_x(\delta\Upsilon)_x dx + \mathcal{E}I\int_0^L \Upsilon_{xx}(\delta\Upsilon)_{xx}dx. \quad (113)$$

Please note that the bottom boundary at $x = 0$ is fixed, and the slope of the riser at this boundary is zero. The variation variable $\delta\Upsilon$ satisfies the conditions $\delta\Upsilon(x,t_0) = \delta\Upsilon(x,t_1) = 0$ and $\delta\Upsilon(0,t) = \delta\Upsilon_x(0,t) = 0$. By applying integration by parts, we can derive from equation (112) that:

$$\int_{t_0}^{t_1}\delta\mathcal{K}(t)dt = -\rho I\int_{t_0}^{t_1}\Upsilon_{xtt}(L,t)\delta\Upsilon(L,t)dt + \int_{t_0}^{t_1}\int_0^L[\rho I\Upsilon_{xxtt} - \rho\Lambda\Upsilon_{tt}]\delta\Upsilon dxdt. \quad (114)$$

Analogously, we can calculate from equation (113) that:

$$\begin{aligned}\int_{t_0}^{t_1}\delta\mathcal{U}(t)dt &= (P-\mathcal{E}\Lambda)\int_{t_0}^{t_1}\frac{\Upsilon_x(L,t)}{\sqrt{1+\Upsilon_x^2(L,t)}}\delta\Upsilon(L,t)dt \\ &+ \int_{t_0}^{t_1}[\mathcal{E}\Lambda\Upsilon_x(L,t) - \mathcal{E}I\Upsilon_{xxx}(L,t)]\delta\Upsilon(L,t)dt \\ &+ \int_{t_0}^{t_1}\int_0^L[-\mathcal{E}\Lambda\Upsilon_{xx} + \mathcal{E}I\Upsilon_{xxxx}]\delta\Upsilon dxdt \\ &- (P-\mathcal{E}\Lambda)\int_{t_0}^{t_1}\int_0^L\Big[\frac{\Upsilon_x}{\sqrt{1+\Upsilon_x^2}}\Big]_x\delta\Upsilon dxdt \\ &+ \mathcal{E}I\int_{t_0}^{t_1}\Upsilon_{xx}(L,t)[\delta\Upsilon(L,t)]_x dt. \end{aligned} \quad (115)$$

By substituting equations (10), (114), and (115) into Hamilton's principle (11), we can demonstrate that

$$\begin{aligned}0 = &\int_{t_0}^{t_1}\Big[U_1(t) - [\mathcal{E}\Lambda + \frac{P-\mathcal{E}\Lambda}{\sqrt{1-\Upsilon^2(L,t)}}]\Upsilon_x(L,t) \\ &-\rho I\Upsilon_{xtt}(L,t) + \mathcal{E}I\Upsilon_{xxx}\Big]\delta\Upsilon(L,t)dt \\ &+\int_{t_0}^{t_1}[U_2(t) - \mathcal{E}I\Upsilon_{xx}(L,t)][\delta\Upsilon(L,t)]_x dt \\ &-\int_{t_0}^{t_1}\int_0^L\Big[\rho\Lambda\Upsilon_{tt} - \rho I\Upsilon_{xxtt} + \mathcal{E}I\Upsilon_{xxxx} \\ &-[(\mathcal{E}\Lambda + \frac{P-\mathcal{E}\Lambda}{\sqrt{1+\Upsilon_x^2}})\Upsilon_x]_x\Big]\delta\Upsilon dxdt.\end{aligned}$$

Given the arbitrariness of the variable $\delta\Upsilon$, we can derive the governing equation (1) and the boundary conditions (5).

References

[1] K. Ammari, A. Bchatnia, and B. Chentouf, "Improved results on the nonlinear feedback stabilisation of a rotating body-beam system," *International Journal of Control*, vol. 95, no. 10, pp. 2726–2733, 2022.

[2] F. Alabau-Boussouira, "A unified approach via convexity for optimal energy decay rates of finite and infinite dimensional vibrating damped systems with applications to semi-discretized vibrating damped systems," *Journal of Differential Equations*, vol. 248, no. 6, pp. 1473–1517, 2010.

[3] F. Alabau-Boussouira and K. Ammari, "Sharp energy estimates for nonlinearly locally damped pdes via observability for the associated undamped system," *Journal of Functional Analysis*, vol. 260, no. 8, pp. 2424–2450, 2011.

[4] F. Alabau-Boussouira, "Convexity and weighted integral inequalities for energy decay rates of nonlinear dissipative hyperbolic systems," *Applied Mathematics and Optimization*, vol. 51, no. 1, pp. 61–105, 2005.

[5] F. Alabau-Boussouira, "Asymptotic behavior for Timoshenko beams subject to a single nonlinear feedback control," *Nonlinear Differential Equations and Applications NoDEA*, vol. 14, pp. 643–669, 2007.

[6] M. Cavalcanti, I. Lasiecka, and D. Toundykov, "Wave equation with damping affecting only a subset of static wentzell boundary is uniformly stable," *Transactions of the American Mathematical Society*, vol. 364, no. 11, pp. 5693–5713, 2012.

[7] M. M. Cavalcanti, V. N. D. Cavalcanti, and I. Lasiecka, "Well-posedness and optimal decay rates for the wave equation with nonlinear boundary damping–source interaction," *Journal of Differential Equations*, vol. 236, no. 2, pp. 407–459, 2007.

[8] Y. Cheng, Y. Li, Y. Wu, and K.-S. Hong, "Anti-disturbance control for a nonlinear flexible beam with velocity disturbance at the boundary," *Automatica*, vol. 152, p. 110978, 2023.

[9] Y. Cheng, B.Z. Guo, and Y. Wu, "Boundary stabilization for axially moving Kirchhoff string under fractional pi control," *Zeitschrift für Angewandte Mathematik und Mechanik*, vol. 102, no. 6, p. e202100524, 2022.

[10] Y. Cheng, Y. Wu, and B.Z. Guo, "Boundary stability criterion for a nonlinear axially moving beam," *IEEE Transactions on Automatic Control*, vol. 67, no. 11, pp. 5714–5729, 2022.

[11] Y. Cheng, Y. Wu, B.Z. Guo and Y. Wu, "Stabilization and decay rate estimation for axially moving Kirchhoff-type beam with rotational inertia under nonlinear boundary feedback controls," *Automatica*, vol. 163, p. 111597, 2024.

[12] Y. Cheng, Y. Wu, and B.Z. Guo, "Absolute boundary stabilization for an axially moving Kirchhoff beam," *Automatica*, vol. 129, p. 109667, 2021.

[13] I. Chueshov, M. Eller, and I. Lasiecka, "On the attractor for a semilinear wave equation with critical exponent and nonlinear boundary dissipation," *Communications in Partial Differential Equations*, pp. 1901–1951, 2002.

[14] K. D. Do, "Boundary control of transverse motion of flexible marine risers under stochastic loads," *Ocean Engineering*, vol. 155, pp. 156–172, 2018.

[15] K. D. Do and J. Pan, "Boundary control of transverse motion of marine risers with actuator dynamics," *Journal of Sound and Vibration*, vol. 318, no. 4-5, pp. 768–791, 2008.

[16] K. D. Do and J. Pan, "Boundary control of three-dimensional inextensible marine risers," *Journal of Sound and Vibration*, vol. 327, no. 3-5, pp. 299–321, 2009.

[17] A. Pazy, *Semigroups of Linear Operators and Applications to Partial Differential Equations,* Springer Science & Business Media, 2012.

[18] M. Fard and S. Sagatun, "Exponential stabilization of a transversely vibrating beam via boundary control," *Journal of Sound and Vibration*, vol. 240, no. 4, pp. 613–622, 2001.

[19] W. He, S. Zhang, and S. S. Ge, "Robust adaptive control of a thruster assisted position mooring system," *Automatica*, vol. 50, no. 7, pp. 1843–1851, 2014.

[20] W. He, S. S. Ge, B. V. E. How, Y. S. Choo, and K.-S. Hong, "Robust adaptive boundary control of a flexible marine riser with vessel dynamics," *Automatica*, vol. 47, no. 4, pp. 722–732, 2011.

[21] B. How, S. Ge, and Y. Choo, "Active control of flexible marine risers," *Journal of Sound and Vibration*, vol. 320, no. 4-5, pp. 758–776, 2009.

[22] W. He, C. Sun, and S. S. Ge, "Top tension control of a flexible marine riser by using integral-barrier lyapunov function," *IEEE/ASME Transactions on Mechatronics*, vol. 20, no. 2, pp. 497–505, 2014.

[23] M. A. Horn and I. Lasiecka, "Global stabilization of a dynamic von Kármán plate with nonlinear boundary feedback," *Applied Mathematics and Optimization*, vol. 31, no. 1, pp. 57–84, 1995.

[24] G. Hegarty and S. Taylor, "Classical solutions of nonlinear beam equations: existence and stabilization," *SIAM Journal on Control and Optimization*, vol. 50, no. 2, pp. 703–719, 2012.

[25] W. M. Haddad and V. Kapila, "Absolute stability criteria for multiple slope-restricted monotonic nonlinearities," *IEEE Transactions on Automatic Control*, vol. 40, no. 2, pp. 361–365, 1995.

[26] T. Hu, B. Huang, and Z. Lin, "Absolute stability with a generalized sector condition," *IEEE Transactions on Automatic Control*, vol. 49, no. 4, pp. 535–548, 2004.

[27] J. Lagnese and G. Leugering, "Uniform stabilization of a nonlinear beam by nonlinear boundary feedback," *Journal of Differential Equations*, vol. 91, no. 2, pp. 355–388, 1991.

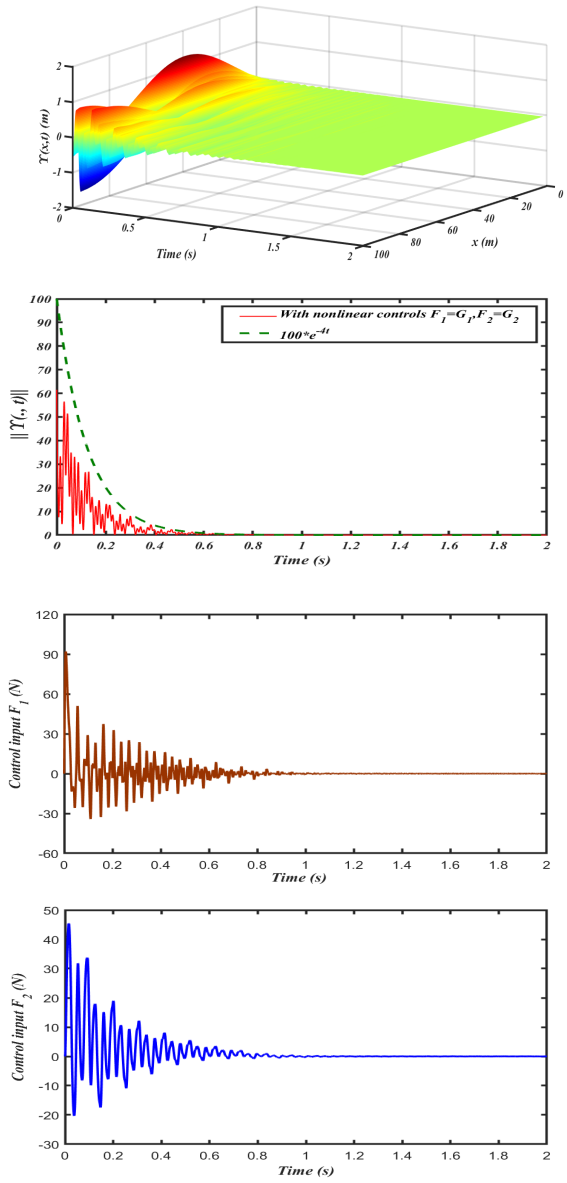

Fig. 5. Transverse displacements and norm $\|\Upsilon(\cdot,t)\|$ of the closed-loop system with the control inputs $F_1 = G_1$ and $F_2 = G_2$.

[28] T.C. Li, Z.C. Hou, and J.F. Li, "Stabilization analysis of a generalized nonlinear axially moving string by boundary velocity feedback,"*Automatica*, vol. 44, no. 2, pp. 498–503, 2008.

[29] U. Lee and I. Jang, "On the boundary conditions for axially moving beams," *Journal of Sound and Vibration*, vol. 306, no. 3-5, pp. 675–690, 2007.

[30] I. Lasiecka and D. Tataru, "Uniform boundary stabilization of semilinear wave equations with nonlinear boundary damping," *Differential and integral Equations*, vol. 6, no. 3, pp. 507–533, 1993.

[31] W. J. Liu and E. Zuazua, "Decay rates for dissipative wave equations," *Ricerche di Matematica*, vol. 48, no. 240, pp. 61–75, 1999.

[32] P. Martinez, "A new method to obtain decay rate estimates for dissipative systems," *ESAIM: Control, Optimisation and Calculus of Variations*, vol. 4, pp. 419–444, 1999.

[33] T. Nguyen, K. D. Do, and J. Pan, "Global stabilization of marine risers with varying tension and rotational inertia," *Asian Journal of Control*, vol. 16, no. 5, pp. 1448–1458, 2014.

[34] E. Pereira, S. S. Aphale, V. Feliu, and S. R. Moheimani, "Integral resonant control for vibration damping and precise tip-positioning of a single-link flexible manipulator," *IEEE/ASME Transactions on Mechatronics*, vol. 16, no. 2, pp. 232–240, 2010.

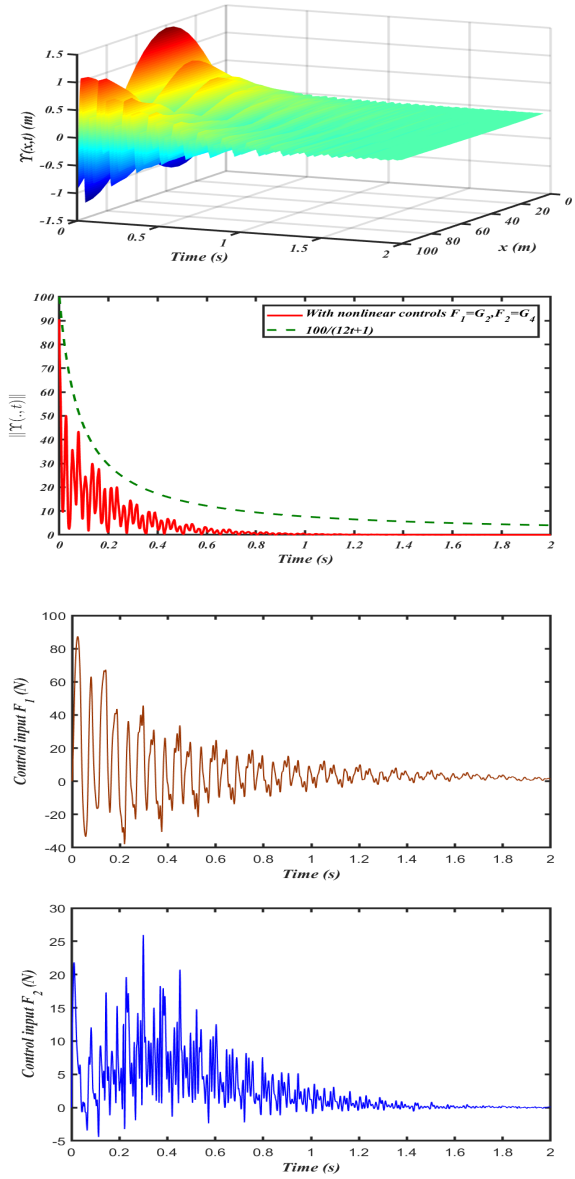

Fig. 6. Transverse displacements and norm $\|\Upsilon(\cdot,t)\|$ of the closed-loop system with the control inputs $F_1 = G_2$ and $F_2 = G_4$.

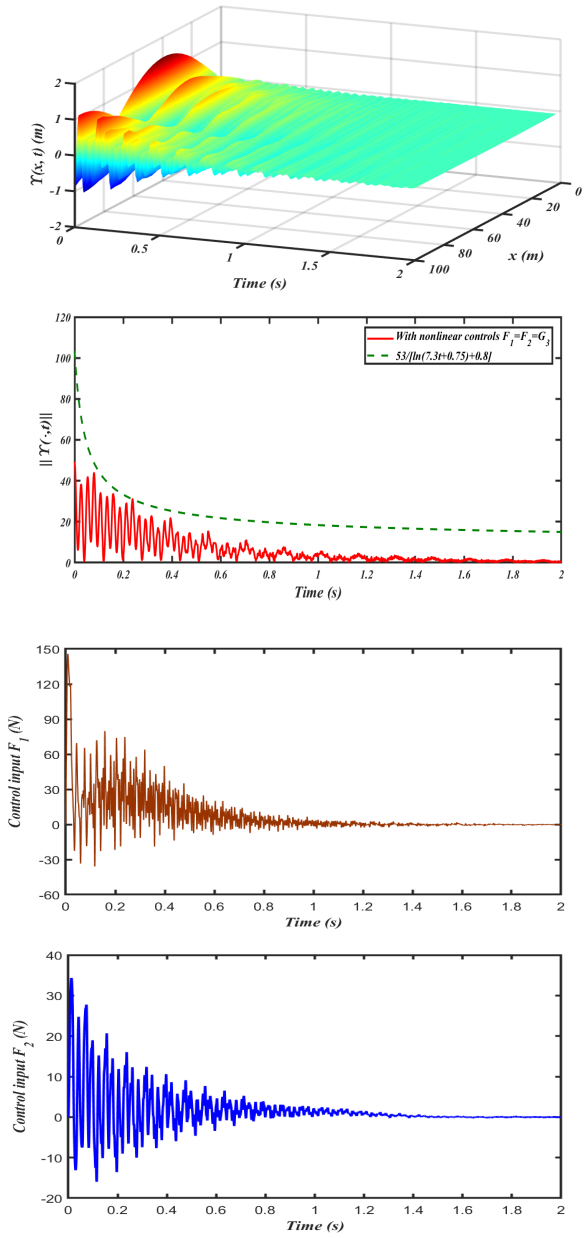

Fig. 7. Transverse displacements and norm $\|\Upsilon(\cdot,t)\|$ of the closed-loop system with the control inputs $F_1 = G_3$ and $F_2 = G_3$.

[35] P. Park, "Stability criteria of sector-and slope-restricted lur'e systems," *IEEE Transactions on Automatic Control*, vol. 47, no. 2, pp. 308–313, 2002.

[36] R. Ramos Jr and C. P. Pesce, "A consistent analytical model to predict the structural behavior of flexible risers subjected to combined loads," *J. Offshore Mech. Arct. Eng.*, vol. 126, no. 2, pp. 141–146, 2004.

[37] B. Rao, "A compact perturbation method for the boundary stabilization of the rayleigh beam equation," *Applied Mathematics and Optimization*, vol. 33, no. 3, pp. 253–264, 1996.

[38] H. Ramirez, H. Zwart, and Y. Le Gorrec, "Stabilization of infinite dimensional port-Hamiltonian systems by nonlinear dynamic boundary control," *Automatica*, vol. 5, pp. 61–69, 2017.

[39] C. Sun, H. Gao, W. He, and Y. Yu, "Fuzzy neural network control of a flexible robotic manipulator using assumed mode method," *IEEE Transactions on Neural Networks and Learning Systems*, vol. 29, no. 11, pp. 5214–5227, 2018.

[40] J. Song, W. Chen, S. Guo, and D. Yan, "LQR control on multimode vortex-induced vibration of flexible riser undergoing shear flow," *Marine Structures*, vol. 79, p. 103047, 2021.

[41] S. Shahruz and D. Kurmaji, "Vibration suppression of a non-linear axially moving string by boundary control," *Journal of Sound and Vibration*, vol. 1, no. 201, pp. 145–152, 1997.

[42] S. Zhang, L. Tang, and Y.-J. Liu, "Output feedback control of a flexible marine riser with the top tension constraint," *Systems & Control Letters*, vol. 163, p. 105208, 2022.

[43] H. C. Zhou, B. Z. Guo, and S. H. Xiang, "Performance output tracking for multidimensional heat equation subject to unmatched disturbance and noncollocated control," *IEEE Transactions on Automatic Control*, vol. 65, no. 5, pp. 1940–1955, 2019.

[44] J. Mawhin, *Critical Point Theory and Hamiltonian Systems,* Springer Science & Business Media, vol. 74, 2013.

Yi Cheng received his M.S. degree in Mathematics from Harbin Institute of Technology, Harbin, China in 2008, and his Ph.D. in Mathematics from Jilin University, Jilin, China in 2013. In 2021, Dr. Cheng attained the position of full professor at Bohai University, Jinzhou, China. His research primarily centers on nonlinear PDE systems and the control of distributed parameter systems.

Yuexi Zhang graduated with a B.S. degree from the School of Mathematical Sciences at Tianjin Normal University, Tianjin, China, in 2020. Currently, she is pursuing an M.S. degree at the School of Science, Bohai University. Her research interests lie in the areas of partial differential equations and the control theory of distributed parameter systems.

Yuhu Wu obtained his PhD degree in Mathematics from Harbin Institute of Technology, Harbin, China, in January 2012. Following this, he served as an assistant professor at Harbin University of Science and Technology, China, from 2012. Between 2012 and 2015, he conducted postdoctoral research at Sophia University, Japan. In 2015, he joined the School of Control Science and Engineering at Dalian University of Technology, China, where he currently holds a professorship. His research interests span non-linear control theory, game theoretic control, as well as applications of control in automotive powertrain systems and unmanned aerial vehicles.

Bao-Zhu Guo obtained his Ph.D. degree in Applied Mathematics from the Chinese University of Hong Kong in 1991. Prior to this, he served as a Research Assistant at Beijing Institute of Information and Control, China, from 1985 to 1987. Between 1993 and 2000, he was affiliated with Beijing Institute of Technology, initially as an associate professor (1993-1998) and later as a full professor (1998-2000). Since 2000, he has been a Research Professor in mathematical system theory at the Academy of Mathematics and Systems Science, Chinese Academy of Sciences. Additionally, since 2019, he has been associated with the School of Mathematics and Physics, North China Electric Power University, Beijing. His primary research focus is on control theory of infinite-dimensional systems.